HEAVY QUARKONIA AND SUPERSYMMETRIC PARTICLES

THESIS SUBMITTED FOR THE DEGREE

OF

DOCTOR OF PHILOSOPHY (SCIENCE)

SUGOPA GHOSH (MONDAL)
DEPARTMENT OF PHYSICS
NORTH BENGAL UNIVERSITY
1990

ST - VERP

To

My Father

Preface

This thesis contains some results of the work done during the last five years in the Department of Physics, North Bengal University. It is a pleasure to express my indebtedness to all those who have been helpful to me in the preparation of this thesis.

I know no words to express my regards and gratitude to my supervisor Professor S. Mukherjee, Head of the Department of Physics, N.B.U., whose guidance, encouragement and suggessions immensely helped me from the very beginning of this work. I am very much grateful to the Indian Space Research Organization for providing me the necessary financial assistance in a project under the RESPOND Programme. I also wish to record my gratitude to all my teachers and seniors in the Dept. of Physics. In particular, I am indebted to Dr. D. P. Datta for his helpful suggestions and to my colleagues, A. K. Roy, B. C. Paul and P. Chakraborty for numerous help. I am also thankful to the staff-members of the University library and the Computer Centre, N.B.U., for providing me all facilities required for the work. I must add special words of appreciation for the support I received from all staff-members of the Physics Department. Finally, I wish to record my gratitude and indebtedness to my mother, Mrs. Chandana Ghosh, for her loving support, encouragement and infinite patience which made it possible for me to write this thesis.

March 26, 1990.

Sugopa Ghosh (Mondal)
Sugopa Ghosh (Mondal)

CONTENTS

* *CHAPTER I*

INTRODUCTION

* This is mostly a review of earlier works.

I.1. Introduction - Background and Objective :

During the last two decades, the developments in particle physics have mostly centred around gauge symmetries of particle interactions. It is now generally believed that Quantum Chromodynamics (QCD), the gauge theory of colour SU(3), describes the strong interactions of particles while the Salam-Weinberg-Glashow $SU(2)_L \times U(1)$ gauge theory describes their weak and electromagnetic interactions. A further step in the direction of finding a complete and fundamental law for particle interaction will be to try to unify these forces. An intensive study of QCD and the interquark interaction, in particular, may provide useful information in our quest for a successful theory of unification. The recently discovered quarkonium states present objects of great interest in this connection.

The quarkonium spectroscopy provides a field where the concepts of QCD could be tested experimentally. Deep-Inelastic Lepton scattering processes have already provided some confirmation of the perturbative QCD. The quarkonium spectroscopy has the potential of becoming another field, within the range of our experimental capabilities, where QCD may be tested qualitatively at all distance scales. The results obtained so far tend to confirm the expectation that QCD is the most promising candidate for a dynamical theory of strong interactions. It is a non-abelian local gauge theory which describes the interaction of quarks with

massless coloured spin 1 gauge bosons, the gluons. Unlike in QED, the effective coupling constant in QCD becomes feeble at large momentum transfers (at short-distances), so that quarks no longer interact strongly at small interquark separations. This concept of asymptotic freedom[1] is consistent with the deep-inelastic scattering results.[2] In QCD, the three colours of a quark are assumed to transform as a fundamental representation whereas the gluons transform as an adjoint representation of $SU(3)_c$. An important constraint on the theory is that elementary coloured quarks and gluons are not directly observable in an experiment. Thus the observed bound states are supposed to be singlets in the colour space.

In QCD calculations, the results of a perturbation theory are expected to be accurate for large momentum transfers. Since the effective quark gluon coupling becomes small at high energies, the one-gluon-exchange term dominates the potential and the interaction potential is roughly of the coulomb type $V(r) \sim 1/r$. However, perturbative QCD does not give any explanation of the quark confinement. The general expectation is that at a large separation, quarks feel an increasingly strong restoring force which is responsible for their confinement. The Confining hypothesis now seems to be an essential ingradient for building models of quarkonia. The interaction is supposed to guarantee that all hadronic states observable in nature are colour singlets. The large distance part of the potential is, however, not yet determined accurately. Its behavior may be as given by the

string[3] and flux-tube[4] models. Lattice gauge theories[5] provide some useful guidance here. It is not yet clear whether the rate of growth of the potential is logarithmic[6] or some power[7,8] of distance. A popular belief is that the potential rises linearly with the inter-quark distance, *i.e.* $V(r) \sim kr$ where k is the string constant, a behavior also expected from Wilson's area law. While the choice of the long distance potential gets some guidance from our theoretical bias, practically not much is known about the nature of the potential in the intermediate range. This is where the heavy quarkonium spectroscopy proves to be useful. The spectroscopy carries information about the shape of the potential at all distances, including the cross-over region, *i.e.* in the gap between the one-gluon-exchange potential and the confining potential.

It may be recalled that the existence of five flavours of quarks (u,d,c,s,b) has so far been found to be consistent with the experimental results. However, on theoretical grounds, a sixth massive quark (top quark) is essential for the standard three gereration model.[9] Although the top quark is yet to be discovered, the search is on, particularly for the toponium states, which would have properties similar to ψ and Υ systems. All these states should be described fairly accurately by the Schrödinger equation with a flavour independent non-relativistic potential $V(r)$.[10] Since the mass of the quark is assumed to be large compared to its binding energy, the relativistic effects should give only small corrections.

To test the concepts outlined above, one has to calculate the energy levels, leptonic decay widths as well as E1 transition rates for heavy quarkonia by considering the spin-independent potential as the sum of the short and long-range potentials. We have undertaken a similar study in chapter II. As a first step, we have considered a non-relativistic potential consisting of a short-range 2-loop QCD potential matched to a confining potential at a large distance. Apart from the $c\bar{c}$ and $b\bar{b}$ states, we have also studied the postulated $t\bar{t}$ states using the same flavour independent potential. We repeated the calculations including the relativistic corrections. We have noted that the standard Breit-Fermi type of spin-dependent potentials cannot satisfactorily explain the fine-hyperfine splittings of heavy quarkonium states. The recent observations of $^1P_1$ states of the $b\bar{b}$ and $c\bar{c}$ families have sharply focussed on the limitations of the standard potentials. In chapter III, we have tried to fit the experimental results by considering an additional contribution to the fine-hyperfine interaction potentials staying within the framework of Breit-Fermi form. In chapter IV, we have made use of the general properties of Schrödinger equation to predict some results for the wave-function at the origin pertaining to $^3S_1$ and $^1S_0$ states of $Q\bar{Q}$ systems. In the last chapter, using a similar technique, some useful results for the two gluino bound states have also been obtained by making use of supersymmetry (SUSY).

The aim of this thesis was to study the properties of some newly discovered mesons which are identified as bound states of a

heavy quark and its antiparticle so as to obtain some constraints on QCD. Considerable phenomenological studies have already been made in this field but this rapidly developing area of studies make it necessary that our theoretical results be continuously compared with new experimental results. The phenomenology of heavy quarkonia provides tests for the entire model based on QCD, the standard electroweak theory and other theoretical ideas of particle interactions. Using SUSY as an additional input, we could study the two gluino bound states within the same formalism. Our results on $\tilde{g}\tilde{g}$ bound states will be useful in the confirmation of both QCD and SUSY and in establishing the interplay between the two most appealing theoretical ingradients of high energy physics.

II.2. Heavy Quarkonia - Experimental Results :

Considerable experimental results are now available for a detailed study of quarkonium spectroscopy. The spectroscopic notation for a $Q\bar{Q}$ level is denoted by $n^{2S+1}L_J$ where the symbols have their usual meaning. The two spin-half quarks can form spin-singlet and spin-triplet states. The $^3S_1$ state with L=0 is split into $^3S_1$ and $^1S_0$ states. For $L \geq 1$, one expects four states $^3L_{L-1}$, ^3L_L , $^3L_{L+1}$ and $^1L_1$ which become non-degenerate due to fine-hyperfine interactions. Some states have already been discovered.

Electron-positron colliders are well-suited for the study of heavy quarkonia. The triplet S-states are produced directly in

e^+e^- annihilations whereas other states are produced via electromagnetic and hadronic transitions. The present experimental information about the S-states , P-states and their radial excitations for $b\bar{b}$ and $c\bar{c}$ systems are presented below.

Four $b\bar{b}$ resonance, Υ,[11] Υ',[12,13] Υ''[12] and Υ'''[14] have been observed in e^+e^- annihilation. But no singlet S-state (η_b) and $b\bar{b}(^3D_1)$ state have so far been seen. Four experiments, *i.e.* CUSB,[15] CLEO,[16] ARGUS[17] and Crystal Ball[18,19] detectors have observed the 1^3P_J states from the radiative decays of $\Upsilon(2S)$. Each group confirmed the existence of χ^1 and χ^2 states. But some discrepancy in the mass of χ^0 state has been reported. However, the mass value reported by ARGUS is possibly more reliable because of their accurate measurement of photon energy. The existence of 2P bound states $\chi_b'^J$ have been reported by CUSB group[20] while the spin-singlet P-state in bottomonium, h_b, has been reported by CLEO Collaboration.[21]

The charmonium states ψ and ψ' have been observed in $p\bar{p}$ annihilation.[22] Subsequently, further states, *viz.* η_c, χ_c^1 and χ_c^2 states were also observed in $p\bar{p}$ annihilation by the R704 Collaboration.[23] Gaiser *et al.*[24] have measured the masses of χ_c^J states by studying the process $\psi(2S) \to \gamma\chi$. The η_c state has been detected[24] in the inclusive photon spectra of both ψ and ψ'. In addition, another paracharmonium state η_c' has been discovered by the Crystal Ball group.[25] The $\psi(^3D_1)$ state[26] has also been observed in the e^+e^- cross-section. The R704 Collaboration[27] has reported some preliminary results about the

spin-singlet state h_c which lies below the ψ' level. A review of particle properties by Particle Data Groups[28] gives us the experimental information for different states of the quarkonium systems. The masses of all the confirmed levels have been shown in Table 3.3 and Table 3.4. So far there is no signature of a toponium and the general belief is that the mass of the top quark, if it exists, should be much higher[74] than 30-50 GeV, as anticipated by UA1 Collaboration.[29] The aspects of the quarkonium spectroscopy which are usually studied are discussed breifly in the following :

i) Masses of quarks and quarkonia :

The mass spectrum of a quarkonium family is given by

$$M_n(Q\bar{Q}) = 2M_Q + E_n(M_Q,V) \qquad (1.1)$$

where M_Q is the quark mass and E_n is the energy eigenvalue of the non-relativistic Schrödinger equation with the chosen $Q\bar{Q}$ potential V(r). The input mass in this calculation is the mass assigned to the relevant quark flavour. Since free quarks have not yet been seen, it is difficult to measure its mass in the usual way. The quark masses are known indirectly from measurements on hadrons and different measurements may, in principle, lead to different masses. Two different types of masses are usually associated with the quark of a given flavour, the current mass and the constituent mass. The processes involving large momentum transfers are associated with the current mass. For dealing with the static

properties of hadrons, constituent mass is more suitable. It may be noted that inside the hadron, quarks are associated with gluon field. An alternative defination of the constituent quark mass is that it minimizes the effects of gluons and sea quarks in a calculation of the static properties. However, the constituent quark masses are usually treated as free parameters in a potential model calculation of the quarkonium.

ii) Leptonic Width :

The leptonic decay mode of a vector meson is due to $Q\bar{Q}$ annihilation via a virtual photon. The non-relativistic formula for the decay of a quark-antiquark bound state into a lepton pair[30] is

$$\Gamma_{ee} = \frac{4\, e_Q^2\, \alpha^2}{M_{Q\bar{Q}}^2} \left|\phi(0)\right|^2 \quad . \qquad (1.2)$$

Thus the annihilation amplitude is proportional to $\phi(0)$, the value of the wave-function of the $Q\bar{Q}$ state at zero separation. The formula should, however, be corrected for vacuum polarization effect, which has been treated by a number of authors.[31] In most cases the correction may be included by following the suggestion of Poggio and Schnitzer, *viz.* by replacing $\phi(0)$ by $\phi(1/M_Q)$, where M_Q is the quark mass. Physically this expresses the simple fact that the annihilation may take place once the particles are within the de-Broglie wavelengths of each other. The measured leptonic

widths of the heavy quarkonia provide useful constraints on the wave-function and hence on the $Q\bar{Q}$ potential.

iii) E1 Transitions :

The transitions of heavier quarkonia to lighter ones take place through either strong or electromagnetic interaction. Some of the electromagnetic transitions which have been observed are $1^3P_J \to 1^3S_1$, $2^3P_J \to 1^3S_1$, $2^3S_1 \to 1^3P_J$, $2^3P_J \to 2^3S_1$, $3^3S_1 \to 1^3P_J$ and $3^3S_1 \to 2^3P_J$. These are all E1 transitions. Some M1 transitions have also been observed but this will not be treated here. The quarkonium wave-function which is approximately determined by the potential model calculation helps in the evaluation of the relevant decay width, Γ_{E1}. The E1 transition rates of the quarkonia are given by

$$\Gamma(n^3P_J \to \gamma + n'^3S_1) = \frac{4}{9}\,\alpha\, e_Q^2\, \omega^3 \left(\int_0^\infty R_{n0} R_{n'1} r^3 dr \right)^2 , \qquad (1.3)$$

$$\Gamma(n^3S_1 \to \gamma + n'^3P_J) = \frac{4}{3}\,\frac{2J+1}{9}\,\alpha\, e_Q^2\, \omega^3 \left(\int_0^\infty R_{n0} R_{n'1} r^3 dr \right)^2 \qquad (1.4)$$

where e_Q is the electric charge of the quark, ω represents the photon energy and R, the radial wave-function. This transition occurs between states with opposite parity and the partial width is proportional to the square of an overlap integral involving the

1P and 1S wave-functions. Thus one can measure the overlap between the two wave-functions from the transition rate.

It is now well-known that the electric dipole transition $\psi' \to \gamma\chi$, is relatively suppressed. A number of factors seem to contribute to this effect. The dipole matrix element is influenced by the relativistic wave-function distortions. The quantity $|\langle\chi|r|\psi'\rangle|^2$ is particularly sensitive to the relativistic corrections. This is because the integral is found to be the sum of the two contributions of opposite sign due to the presence of a node in the 2S wave-function. A shift in the wave-function caused by the relativistic corrections reduce the value of the matrix element. The coupled channel effects[32] for ψ' which also reduce the overlap between its wave-function and that of the P-wave χ state should also be considered. It is important to note that relativistic corrections in the Y system are much smaller than that in the ψ system.

I.3. Heavy Quarkonia - Theoretical aspects :

For heavy quarkonia, a non-relativistic treatment based on a Schrödinger equation with a static potential should be a very good approximation, so far as the spin-averaged properties are concerned. A number of authors have discussed relativistic spin-dependent calculations making use of this non-relativistic potential. The spin-dependent effects have been obtained by inserting the one-gluon-exchange interaction into the relativistic

wave-equation, such as Bethe-Salpeter[33] (BS) equation with a suitable kernel. The Breit-Fermi reduction[34,35] of the BS equation leads to the well-known spin-dependent interaction terms. However, the reduction involves an approximation of the BS equation which essentially reduces it to a non-relativistic Schrödinger equation with correction terms including both spin-dependent and spin-independent terms. One of the many well-known difficulties in the treatment of the BS equation is related to the relative time coordinate. A number of authors[36,37] have solved the BS equation for quarkonium in the 'instantaneous' approximation so that in the centre of mass frame, the relative time coordinate vanishes. This reduces the BS equation to a Salpeter equation.[38] A QCD oriented BS equation has been discussed by Mittal and Mitra[39] in the 'null-plane' approximation in order to obtain the mass-spectra of heavy as well as light quarkonia. Jacobs *et al.*[40] also have considered an 'instantaneous' approximation to solve the BS equation in momentum space with vector and scalar kernels but the results seem to be quite complicated. It may be pointed out that the non-relativistic Schrödinger equation with the usual Breit-Fermi correction terms can be derived from the Breit equation itself.

Eichten and Feinberg[41] have described the spin-dependent forces in heavy quark systems by taking into account the non-abelian nature of QCD and using a gauge invariant formalism. They start from the wilson loop where a 1/M expansion of the quark propagator is inserted. They relate the spin-dependent parts of

the potential to correlation functions of electric and magnetic field strengths. They assume that the colour-magnetic field interactions vanish at a large distance. Assuming that the long-range part of the potential transforms like a Lorentz scalar, it is argued that the confinement is associated with a purely electric term while the hyperfine potential is associated with the magnetic one. Gromes[42] also has claimed that the confining potential must be a scalar. Gromes has obtained an important relation connecting V_1 , V_2 and V , $V = V_2 - V_1$, which follows from the Lorentz invariance of the theory where V_1 and V_2 represent the spin-orbit potentials and V gives the non-relativistic potential. Representing the magnetic field by a space-like loop integral and applying the area law, Gromes arrives at the conclusion that the sign of the spin-orbit term is opposite to that obtained by Eichten and Feinberg[41] and in an earlier paper by Gromes[43] and is identical with that of Buchmüller.[44]

Using a modified Richardson potential instead of linear plus coulomb form, Moxhay and Rosner[45] have included the relativistic corrections to the spin-independent potential. Following the approach of EF, they calculated the energies, leptonic widths and dipole transition rates of ψ and Υ systems. Some consequences of relativistic effects have been discussed by McClary and Byers[46] choosing a scalar potential for the confining potential. The sign of the spin-orbit contribution arising from a scalar potential is the same as proposed by Buchmüllar[44] and Gromes.[42] Pantaleone *et al.*[47] also adopt an approach based on the

work of EF to calculate the spin-dependent corrections to the static QCD potential upto α_s^2 term. They extend the formalism for both equal and unequal masses to obtain spin-dependent terms which contain logarithmic as well as inverse powers of the heavy quark mass.

On the otherhand, Gupta, Radford and Repko[48,49] (GRR) have given a potential which incorporates higher order perturbative corrections to spin-dependent and spin-independent terms of the $Q\bar{Q}$ potential. They have calculated the fine-hyperfine splittings by a perturbative approach. They consider a renormalization scale parameter μ which is fixed by minimizing the effect of higher order terms which occurs in a renormalization group improvement of the potential. Their study reveals that the confining potential may be regarded as the effect of a scalar exchange. Using GRR scheme, Igi and Ono[50] have investigated the properties of $c\bar{c}$ and $b\bar{b}$ states for various values of $\Lambda_{\overline{MS}}$ and observed that the fine-hyperfine interaction is not only sensitive to the choice of the $Q\bar{Q}$ potential but also very sensitive to the value of $\Lambda_{\overline{MS}}$. Fulcher[51] has developed an abbreviated form of GRR scheme which is based on the numerical solution of the Schrödinger equation. He has considered the α_s^2 correction to the static potential but neglected these corrections for the spin-dependent part. He has included a coulomb term in the confinement potential by introducing a join radius, where the running coupling constant stops running. All these modifications yielded better results for the Y system than what one gets in the original GRR potential.

In the GRR renormalization scheme, the perturbative potential not only depends on the renormalization scheme, but also on the renormalization scale parameter. The method generally involves a long calculation. On the otherhand, in the EF approach, the quantity $\Lambda_{\overline{MS}}$ is usually chosen as one of the free parameters. In our calculation, we have followed the EF approach.

I.4. Supersymmetry and bound states :

The supersymmetric theories have been found to offer a very exciting field of research in the context of the unification schemes of the elementary particle interactions. The idea of supersymmetry (SUSY) was initially introduced to solve the gauge hierarchy problem in GUTS. It has also an aesthetic appeal. It is, therefore, not surprising that these theories have opened up a very attractive field of research.

In supersymmetric theories, elementary bosons have supersymmetric fermion partners and vice-versa. The supersymmetric partners have the same mass when SUSY is unbroken. The fermionic and bosonic masses and couplings get related to each other when SUSY is imposed on a theory, thereby reducing the number of free parameters in the theory.

If SUSY is broken, the energy of the lowest lying state need not be exactly zero. One expects SUSY to be approximate in nature, so that the superpartners will be split. One of the important features of a supersymmetric theory is that it predicts

the existence of associated particles differing by one-half unit of spin. Among the SUSY particles, the gluino, the SUSY partner of the gauge boson gluon, seems to offer a wide range of interactions accesible by the present experimental facilities. Each superpartner carries a good quantum number, R-parity,[52] which plays the role of a flavour-conserving quantum number. In almost all models, the gluino is expected to be the lightest sparticle, apart from the photino, the spin 1/2 partner of photon. Photino is expected to be a very light particle and its detection is very much difficult due to its relatively weak interaction. In most models, supersymmetric particles may be detected by their decay products. The gluino decays predominantly via the process $\tilde{g} \rightarrow Q\bar{Q}\,\tilde{\gamma}$ where photino is assumed to be long-lived. The photino carries off energy and momentum which are not detected.

Like gluon, gluino is a colour octet. Due to this nature and its large coupling strength, the cross-section for producton of a gluino pair is twenty times larger than those of the quark pair of equal mass. Since the lifetime is believed to be relatively long, it can possibly be easily identified. The light gluino search can be carried out in Beam dump experiments[53] with beam energy ~ 1 TeV. At a hadron collider, gluino pair production occur via gluon-gluon scattering.[54] The hadron collider is a suitable place for the search of a heavy gluino. The UA1 Collaboration[55] have analysed the E_T data and have concluded that the mass limit of gluino is greater than 53 GeV. Explicit search for gluino of a mass upto 150-200 GeV at the Fermilab Tevatron have been suggested

by different authors.[56] Barnett *et al.*[57] surveyed the decay modes and signatures of gluinos in minimal supersymmetric model. The important features of these decays and their phenomenological implication have also been discussed.

The gluino, being a self-conjugate majorana fermion, may bind with quarks, gluons and other gluinos and form colour singlet bound states. Like ordinary fermion-antifermion states, the parity of gluinonium ($\tilde{g}\tilde{g}$) state is given by $P = -(-1)^L$ and C-parity positive. The binding energy and wave-function at the origin of $\tilde{g}\tilde{g}$ state are large. Since the gluino mass is heavy, the gluinonium state can be described by the non-relativistic potential model as in the $Q\bar{Q}$ system although some differences occur in the case of gluinos. The differences arise mainly because gluinos are majorana fermions and also because they belong to a colour octet. The short-range part of the potential may be represented as $V_{\tilde{g}\tilde{g}}(r) = \frac{9}{4} V_{Q\bar{Q}}(r)$ where 9/4 comes from the ratio of quadratic casimir operators for the adjoint and fundamental representations. This is valid only for the short-range part of the potential. Some authors,[58,59] however, assumed that this relation holds for the entire $\tilde{g}\tilde{g}$ potential. Among other gluino states, the glueballino ($\tilde{g}g$) states may be formed by replacing one gluino in a gluinonium state by one gluon. These states should be experimentally identified more easily than other glue ball states. Mitra and Ono[60] have studied the properties of the glueballino and hybrino ($\tilde{g}Q\bar{Q}$) states by using a BS model. The discovery of any of these states will be extremely exciting.

I.5. Summary of the work done :

The following gives the chapterwise summary of the work reported in the thesis :

a) In chapter II, the properties of the heavy quarkonia have been studied by the non-relativistic potential model. The potential chosen is the vacuum polarization corrected 2-loop QCD potential supplemented by a confining potential. The energy levels, leptonic decay widths with and without Poggio-Schnitzer correction and E1 transition rates of ψ and Υ families are calculated and are found to be in good agreement with the experimental results. The toponium spectroscopy is studied for the expected range of top quark mass (30-70 GeV). Considering the experimental branching ratio, the total width and the hadronic decay width of the χ_b^J states are also determined. Potential model calculations seem to be fairly successful in describing the non-relativistic properties of heavy quarkonia.

b) In chapter III, we discuss the spin-dependent interactions in $Q\bar{Q}$ systems. We note that the newly discovered $^1P_1$ states of $b\bar{b}$ and $c\bar{c}$ systems, in particular, pose serious problems to the standard models. We present an extensive analysis to show that the standard Breit-Fermi type of interactions cannot fit the experimental results accurately. A modification of the formalism is suggested. A model calculation with a realistic potential is carried out. The potential consists of a 2-loop QCD short-range potential and a scalar long-range potential with an additional term, as suggested

by Lüscher and also supported by lattice-gauge results. The energy level splittings are calculated with this potential. The possibility of including the spin-dependent contribution of a pseudo-scalar exchange is also considered. It is seen that although the modified formalism just about accommodates the trend of data for $^1P_1$ states, the Breit-Fermi interactions in general lead to severe constraints on the parameters of the potential when one tries to fit the entire range of quarkonia data. The choice of the Breit-Fermi form for the spin-dependent interactions do not allow enough freedom to fit the recent data on $^1P_1$ levels.

c) In chapter IV, we note that apart from the inadequacy of Breit-Fermi type of interactions for describing the fine-hyperfine splittings of heavy quarkonia, the presence of highly singular terms like $\delta^3(r)$ and $1/r^3$ terms also tend to make the perturbative calculations unreliable. Exact results or bounds, even if weak, will be very useful in this context. Using Martin's techniques, some weak inequalities for the values of the wave-function at the origin for the triplet and singlet S-states have been derived for a large class of $Q\bar{Q}$ potentials, including the recently proposed Gupta's potential. The inequalities could be used to predict bounds for the decay widths of the η_b states. This inequality will be useful in quarkonium spectroscopy.

d) In chapter V, the effect of the long-range confining potential on the two gluino bound states has been studied in a particular potential model. A power law potential has been chosen as the long-range part of the potential. The asymtotically free nature

of QCD suggests that the short-range behavior is due to one-gluon-exchange. From supersymmetric considerations, we may expect that the short-distance part of the $\tilde{g}\tilde{g}$ potential, $V_{\tilde{g}\tilde{g}}$ is 9/4 times the $Q\bar{Q}$ potential, $V_{Q\bar{Q}}$. However, the relation between long-range parts of $V_{\tilde{g}\tilde{g}}$ and $V_{Q\bar{Q}}$ is completely unknown. We have chosen a long-range $V_{\tilde{g}\tilde{g}}$ potential which is β-times the long-range potential for $Q\bar{Q}$ where β lies in the interval $0.5 \leq \beta \leq 3$. We have applied Martin's techniques to derive some useful inequalities for the value of the wave-function at the origin, $\psi_{\tilde{g}\tilde{g}}(0)$, for a general class of potentials. The results are useful for estimating various decay widths and production cross-sections.

To summarize, our calculations seem to confirm that the phenomenology of the heavy quarkonia are in general consistent with the basic concepts of QCD, although some details are yet to be understood. With the new accelerators becoming operational in near future, a more definite conclusion may hopefully be drawn.

CHAPTER II

NON-RELATIVISTIC POTENTIAL

II.2. Introduction :

The discovery of the heavy quarkonia has led to a very active field of research involving the theoretical predictions of the QCD and some inspired phenomenology guided by the experimental results. Considerable progress has already been made in understanding the properties of these $Q\bar{Q}$ states, considered to be bound by a flavour-independent non-relativistic potential. The observed spin-averaged properties of heavy quarkonia could be explained by different authors with varying degrees of success. However, recent measurement of the fine-hyperfine interactions have led to renewed activities in this field, particularly because the earlier parameters are found to be inadequate. We have considered in this chapter a non-relativistic potential model to study the spectroscopy of heavy quarkonia, particularly those which do not require a relativistic treatment. The study will provide the basic structure for incorporating the relativistic corrections, in particular, the fine-hyperfine interactions, which will be considered in the next chapter. While choosing a potential for the $Q\bar{Q}$ system, we expect the perturbative QCD to be valid at short-distances, while at large distances, a confining potential, possibly a linear one (or a little modification thereof) should be adequate. We have, therefore, considered in this chapter a static potential which consists of a short-range 2-loop QCD potential which is matched to a modified linear potential for

large distances. We have studied in detail the $b\bar{b}$ and $c\bar{c}$ systems. Since the $Q\bar{Q}$ potential is assumed to be flavour independent, the same potential is used to study the toponium states also for a range of possible t-quark masses. The study of toponium is important particularly because the toponium states probe effectively a very short-distance part of the $Q\bar{Q}$ potential which is not probed accurately by the $b\bar{b}$ and $c\bar{c}$ systems. The toponium may provide a possible method of production of the Higgs particle through the decay $T \to H + \gamma$ if allowed kinematically. Lastly, the toponium may provide us with signatures for theories beyond the standard model, in particular, in our search for sparticles.

The scheme of presentation is as follows. In section II.2, we discuss breifly the non-relativistic $Q\bar{Q}$ potential we have taken to calculate the spectroscopy. Calculations of spin-averaged mass spectrum, leptonic decay widths, E1 transition rates of $b\bar{b}$ and $c\bar{c}$ mesons have been done by solving the Schrödinger equation numerically. Various bounds on $t\bar{t}$ quarkonium mass are discussed in section II.3. The predicted energy levels of $t\bar{t}$ systems are also given. By making use of the experimental branching ratio, the total width and hadronic decay width of χ_b^J state are predicted in section II.4. Section II.5 contains some concluding remarks.

II.2. Non-relativistic $Q\bar{Q}$ potential :

The extensive work on the $c\bar{c}$ and $b\bar{b}$ spectroscopy has helped in determining uniquely the $Q\bar{Q}$ static potential within the

range $0.1 \text{ fm} \lesssim r \lesssim 1 \text{ fm}$. In fact, the different potentials[6,61] that fit the spin-averaged data reasonably well all agree within this range. For small distances, the $Q\bar{Q}$ potential should be given accurately by the one-gluon-exchange term with a running coupling constant. This potential upto 2-loop corrections has been considered by a number of authors.[2,62] We, however, make a special choice for the non-relativistic $Q\bar{Q}$ potential

$$V_{Q\bar{Q}}(r) = f(r)V_{QCD}(r) + \left(1 - f(r) \right)V_L(r) \ , \qquad (2.1)$$

where $V_{QCD}(r)$ is the 2-loop QCD potential, V_L is the long-range potential and $f(r)$ is the Woods-Saxon function

$$f(r) = \frac{1 + e^{-r_0/s}}{1 + e^{(r - r_0)/s}} \ . \qquad (2.2)$$

The 2-loop QCD potential, $V_{QCD}(r)$ may be written as[63,76]

$$V_{QCD}(r) = - \frac{4\pi \ C_2(R)}{b_0 \ r \ \ln(1/\Lambda^2_{\overline{MS}} \ r^2)} \left[1 + (2\gamma_E + c/b_0) \frac{1}{\ln(1/\Lambda^2_{\overline{MS}} \ r^2)} \right.$$

$$\left. - \frac{b_1}{b_0^2} \frac{\ln \ln(1/\Lambda^2_{\overline{MS}} \ r^2)}{\ln(1/\Lambda^2_{\overline{MS}} \ r^2)} \right] . \qquad (2.3)$$

In above, γ_E is the Euler constant and

$$b_0 = \frac{11}{3} \ C_2(G) - \frac{2}{3} \ N_f$$

$$b_1 = \frac{34}{3}\left[C_2(G) \right]^2 - \frac{10}{3} C_2(G)\, N_f - 2C_2(R)\, N_f$$

$$c = \frac{31}{9} C_2(G) - \frac{10}{9} N_f \ .$$

In above, $C_2(R)$ and $C_2(G)$ are the invariant quadratic casimir operators, which for $SU(3)_c$ equal 4/3 and 3 respectively. N_f gives the number of quark flavours relevant for the problem, which we choose to be equal to 4. In the standard $\overline{MS}$ scheme, it is customary to choose N_f as the number of quark flavours with mass $\leq \mu$, where μ gives the renormalization scale.

For the long-range potential, we choose the form

$$V_L(r) = Ar + B \left(\ln \Lambda_{\overline{MS}}\, r + 1 \right) \ . \qquad (2.4)$$

We have included the logarithmic term to take into account a small modification of the linear potential. The reason for the choice will be explained in the next chapter. The Woods-Saxon function interpolates smoothly between the short-range potential and the long-range part. The position and the extension of the cross-over region can be fixed by varying the parameters r_0 and s. However, the variation of s is limited within a narrow range, since the cross-over region is approximately known. Combinations of different potentials have been studied by several authors.[64,65] We have followed, in particular, Igi and Hikasa.[63]

We have solved numerically the Schrödinger equation with potential (2.1). We have developed a comprehensive computer

programme for the relevant calculations. We have chosen $\Lambda_{\overline{MS}}$ = 0.196 GeV, M_b = 4.783 GeV and M_c = 1.364 GeV respectively. Bound state masses of $Q\bar{Q}$ systems are obtained from Eq.(1.1) of the first chapter. The parameters of the potential giving the best fit are r_0 = 0.105 fm , s = 0.02 fm, A= 0.019 GeV^2, B = 0.677 GeV. Since no spin-dependent interactions are considered in this chapter, a direct comparison with experimental results is not always possible. Thus the calculated spin-averaged 1S state of $b\bar{b}$ has a mass of 9445.5 MeV while experimental value for $^3S_1$ state is 9460.32 ± 0.22 MeV. The other state $^1S_0$ has not yet been discovered. The problem will be taken up in the next chapter. The agreement with the experimental result is reasonably good. In Ref.(66), the authors have matched the 1S levels with the experimental value without performing fine-hyperfine calculations. It is, however, expected that the inclusion of the fine-hyperfine contribution will shift the energy levels upwards. In that case, the input quark masses will have to be adjusted for better agreement. For the $c\bar{c}$ system, we vary the input c-quark mass so as to obtain the spin-averaged masses. This gives $M_{1S}(c\bar{c})$ = 3068.7 MeV and $M_{2S}(c\bar{c})$ = 3662.8 MeV respectively. The experimental results for these states, determined very accurately, are $M_{1S}(c\bar{c})$ = 3067.93 ± 1.16 MeV and $M_{2S}(c\bar{c})$ = 3663 ± 1.15 MeV, giving an excellent agreement. In Table 2.1, the spin-averaged masses for $b\bar{b}$ and $c\bar{c}$ systems are shown. However, in the case of 1P and 2P states of $b\bar{b}$, we can compare only the centre of gravity mass values. The value of 1P state is shifted downwards by about 15 MeV

Table 2.1. Calculated energy values of the $b\bar{b}$ and $c\bar{c}$ states.

Bound state	Spin-averaged mass of $b\bar{b}$ system(MeV)	Spin-averaged mass of $c\bar{c}$ system(MeV)
1S	9445.5	3068.7
2S	10030.0	3662.8
3S	10358.0	4009.6
4S	10593.0	4265.6
1P	9885.8	3505.2
2P	10257.0	3897.1
1D	10155.0	3784.0
2D	10433.0	4083.0

for both the flavours. The reason for this shift will be discussed later on. In Figs. 2.1, 2.2 and 2.3, we show the variation of the energy difference as a function of $\Lambda_{\overline{MS}}$, r_o and s. We represent the differences as Δ_1 and Δ_2 where Δ_1 = E(1P) - E(1S) and Δ_2= E(2P)- E(1S) respectively.

We have also calculated the leptonic decay widths and E1 transition rates of heavy quarkonia. In calculating the leptonic width we included the Poggio-Schnitzer (PS) correction to the Van-Royen-Weisskopf formula, given in the first chapter. The leptonic widths along with the PS correction are presented in the Table 2.2. It is seen that the value of PS correction factor for the $c\bar{c}$ and $b\bar{b}$ systems is about 0.4 to 0.8. As can be seen from Table 2.2, the results for $c\bar{c}$ system with PS correction are in better agreement with the experimental values. However, in the case of $b\bar{b}$ states, it is clear that the PS correction is not necessary. This is expected, as for $b\bar{b}$ systems, the relevant distance scales are such that the 2-loop QCD potential, which already incorporates the vacuum polarization effect is dominant and no further correction is required.

The E1 transition rates of heavy quarkonia between an initial state i and a final state f are given by the Eqs. (1.3) and (1.4). The photon energy ω may be expressed as

$$\omega = \frac{M^2(v_1) - M^2(v_2)}{2M(v_1)} \quad , \quad M(v_1) > M(v_2) \; . \qquad (2.5)$$

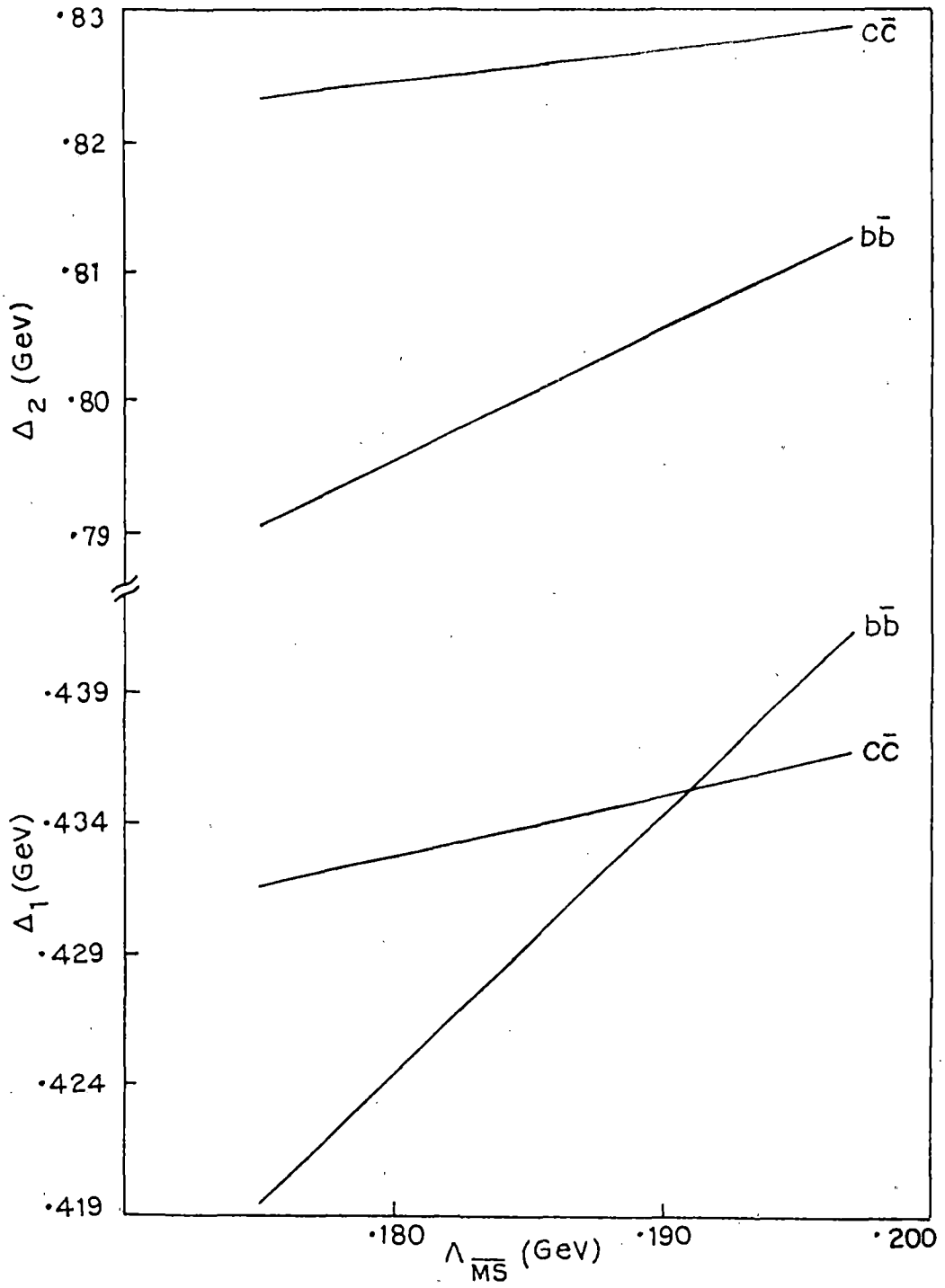

Fig.2.1. Variation of $\Delta_1 = E(1P) - E(1S)$ and $\Delta_2 = E(2P) - E(1S)$ with $\Lambda_{\overline{MS}}$.

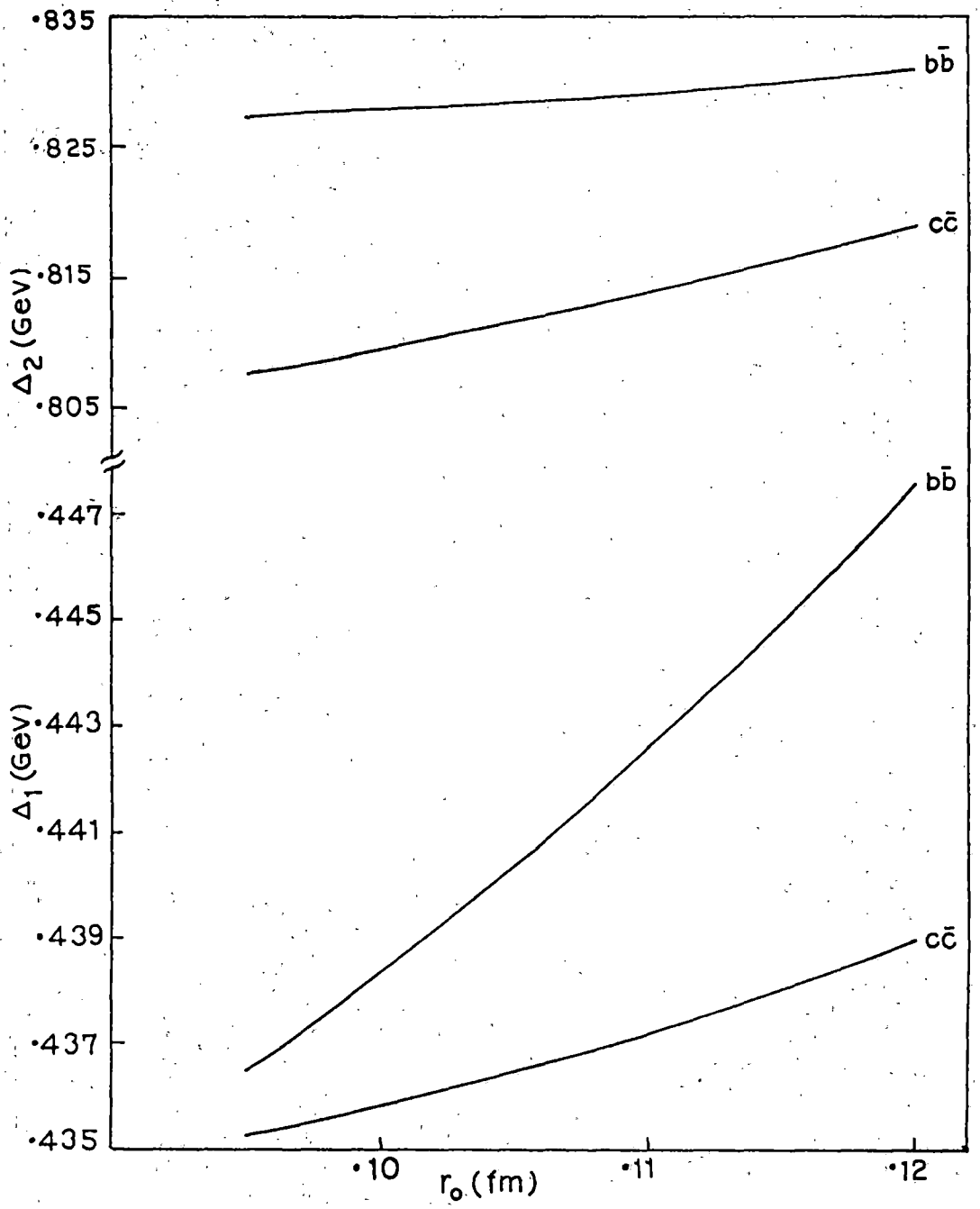

Fig.2.2. Variation of $\Delta_1 = E(1P) - E(1S)$ and $\Delta_2 = E(2P) - E(1S)$ with r_o .

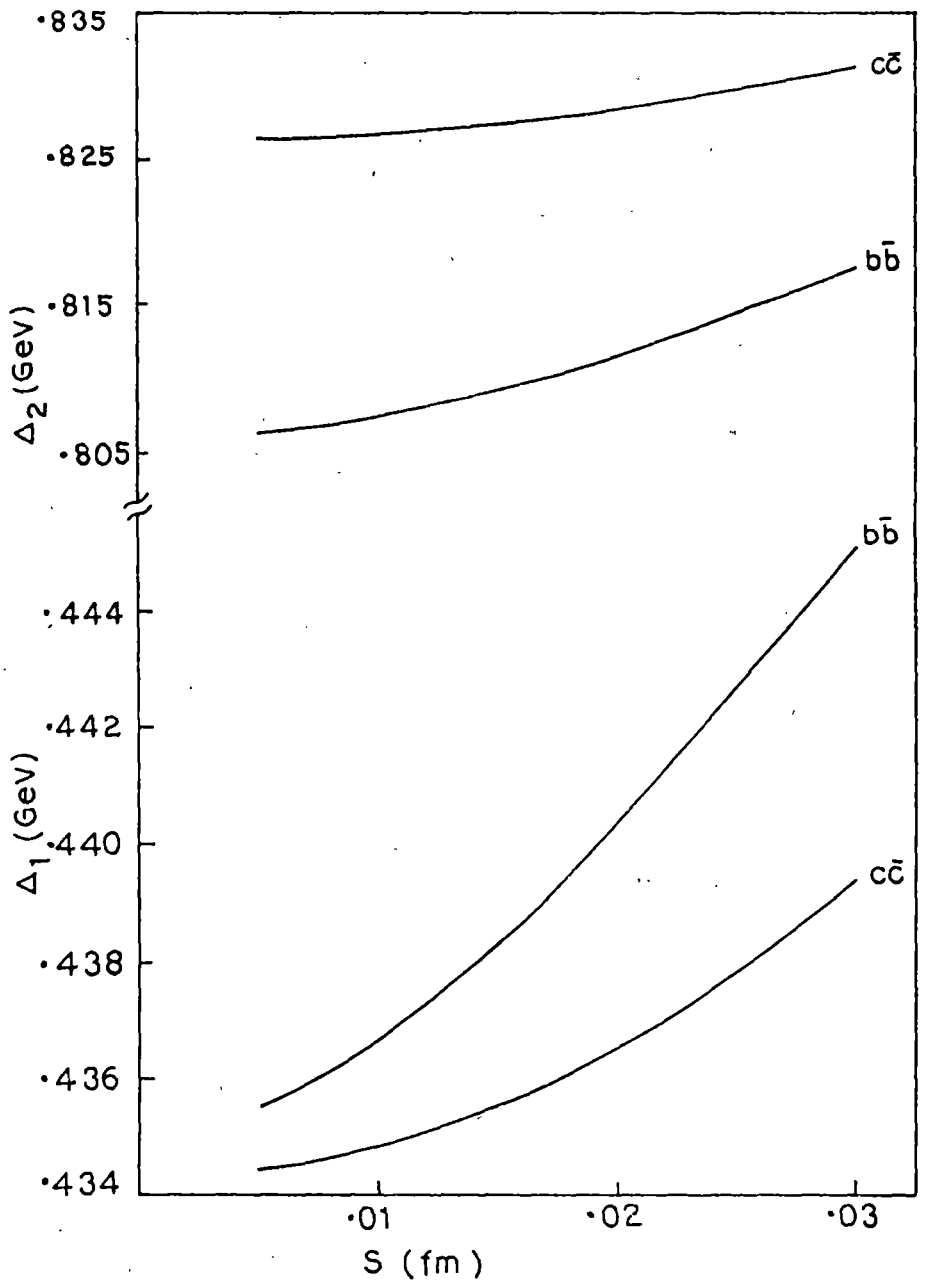

Fig.2.3. Variation of $\Delta_1 = E(1P) - E(1S)$ and $\Delta_2 = E(2P) - E(1S)$ with s .

Table 2.2. Predicted leptonic decay widths of $b\bar{b}$ and $c\bar{c}$ systems without and with Poggio-Schnitzer corrections. Experimental values are taken from Ref.(28).

State	$\lvert \phi(0) \rvert^2$ (GeV^3)	Experimental (KeV)	Uncorrected (KeV)	Poggio-Schnitzer corrected (KeV)
Y(9.460)	5.1738	1.34 ± 0.05	1.373	1.087
Y(10.023)	2.5943	0.60 ± 0.036	0.611	0.462
Y(10.355)	1.8058	0.44 ± 0.03	0.398	0.294
Y(10.580)	1.4192	0.24 ± 0.05	0.299	0.217
ψ(3.097)	0.7088	4.72 ± 0.35	7.127	4.559
ψ(3.685)	0.3832	2.14 ± 0.21	2.704	1.468
ψ(4.040)	0.2766	0.75 ± 0.15	1.629	0.801
ψ(4.415)	0.2327	0.47 ± 0.10	1.211	0.553

Since we have not considered the fine-hyperfine structure in this chapter, we calculate this rates using available experimental values of ω. We have given our results in Table 2.3 and 2.4. We compare our results with the results of some other workers.[51,67,45] Kwong *et al.*[67] used the inverse scattering method to construct the $Q\bar{Q}$ potential. Our results almost agree with the results of the models of Ref. (51) and (67). We have also shown in Table 2.5 the values of the electric dipole matrix elements which are evaluated non-relativistically. The transition rates of $3S \rightarrow 1P$ for $b\bar{b}$ system are very small due to cancellations in the overlap integral for the 3S and 1P wave-functions. This point was also mentioned by Fulcher.[68] In case of $c\bar{c}$, we obtain higher values than the observed rates. This is because the relativistic effects are more important for $c\bar{c}$ than for $b\bar{b}$ system and the relativistic correction is very important for these transition rates.

II.3. t-quark mass and Toponium :

Recent experimental results indicate that the mass of the top quark does not lie around 50 GeV as suggested earlier by the UA1 experimental group at CERN.[29] However, some suitable signatures for detection of the t-quark have been identified[69] recently. One now expects direct as well as indirect signals for the presence of t-quark in the next generation collider energy range, if not earlier. The indirect evidence for a t-quark comes

Table 2.3. E1 transition rates for $b\bar{b}$ system. Experimental values of ω are taken from Ref.(28).

Transition	Experimental ω (MeV)	Transition width (KeV)				Experimental width (KeV)
		MR[45]	FUL[51]	KR[67]	OURS	
$2^3S_1 \rightarrow 1^3P_0$	162.3 ± 1.3	1.0	1.38	1.39	1.277	1.29 ± 0.31
1^3P_1	130.6 ± 0.7	2.1	2.17	2.18	2.000	2.01 ± 0.49
1^3P_2	109.6 ± 0.6	2.2	2.13	2.14	1.966	1.98 ± 0.48
$3^3S_1 \rightarrow 1^3P_0$	483.8 ± 1.4	0.025	0.005	0.007	0.010	
1^3P_1	453.2 ± 0.9	0.025	0.011	0.017	0.026	0.04 ± 0.03
1^3P_2	432.8 ± 0.8	0.15	0.016	0.025	0.037	0.06 ± 0.05
$3^3S_1 \rightarrow 2^3P_0$	119.3 ± 1.1	1.4	1.35	1.65	1.475	1.22 ± 0.3
2^3P_1	99.6 ± 0.4	2.8	2.36	2.52	2.575	3.08 ± 0.6
2^3P_2	85.9 ± 0.7	2.7	2.53	2.78	2.753	3.26 ± 0.7
$1^3P_0 \rightarrow 1^3S_1$	391.7 ± 1.3	31	30.8	26.1	27.917	
1^3P_1	422.5 ± 0.7	36	38.6	32.8	35.034	
1^3P_2	442.9 ± 0.6	38	44.5	37.8	40.357	
$2^3P_0 \rightarrow 1^3S_1$	741.5 ± 2.3	7.5	7.62	8.48	6.744	
2^3P_1	764.8 ± 0.8	12	8.19	9.31	7.400	
2^3P_2	776.8 ± 0.7	14	8.60	9.75	7.753	
$2^3P_0 \rightarrow 2^3S_1$	205.0 ± 2.3	12	13.0	11.3	12.390	
2^3P_1	229.7 ± 0.9	14	17.0	15.9	17.430	
2^3P_2	242.3 ± 0.8	16	20.1	18.7	20.459	

Table 2.4. E1 transition rates for $c\bar{c}$ system. Experimental values of ω are used.

Transition	Experimental ω (MeV)	Transition width (KeV)	
		MR[45]	OURS
$1^3P_0 \rightarrow 1^3S_1$	303.2	226	186.33
1^3P_1	388.7	460	392.60
1^3P_2	429.4	609	529.28
$2^3S_1 \rightarrow 1^3P_0$	261.0	37	69.83
1^3P_1	171.8	48	59.75
1^3P_2	127.7	41	40.90

Table 2.5. Dipole matrix element $\langle r \rangle = \int R\, R' r^3\, dr$ for $b\bar{b}$ and $c\bar{c}$ systems.

Transition	$\langle r \rangle$ (GeV^{-1}) $(b\bar{b})$				$\langle r \rangle$ (GeV^{-1}) $(c\bar{c})$	
	FUL[51]	KR[67]	MR[45]	OURS	MR[45]	OURS
$1^3P_J \rightarrow 1^3S_1$	1.194	1.098	1.08	1.135	2.08	2.15
$2^3S_1 \rightarrow 1^3P_J$	-1.644	-1.646	1.64	-1.577	2.65	-2.86
$2^3P_J \rightarrow 1^3S_1$	0.226	0.240	0.26	0.214		0.37
$2^3P_J \rightarrow 2^3S_1$	1.970	1.911	1.89	1.998		3.72
$3^3S_1 \rightarrow 1^3P_J$	0.0185	0.023	-0.024	-0.028		-0.07
$3^3S_1 \rightarrow 2^3P_J$	-2.573	-2.672	2.68	-2.689		-4.83

from the observed forward-backward asymmetry in $e^+e^- \rightarrow \bar{b}b$ as well as the absence of flavour changing neutral decay of b quark. The indirect constraints $40 < M_t < 200$ GeV on the top quark mass are available from i) the radiative correction to W and Z boson masses and ii) the $B_d - \bar{B}_d$ mixing. A direct quark search, on the otherhand, may be available in the e^+e^- collider although the current energy range is rather low. The data from PETRA and TRISTAN[70] suggest $M_t > 26$ GeV. The next generation LEPI and LEPII colliders are expected to probe t-quark mass upto 50 GeV and 100 GeV respectively. The $p\bar{p}$ colliders seem to be more promising in this respect because of their high energy reach. However, the corresponding t-signal is not very clean and one has to use isolated electron (muon) signature.[71] The current data from the CERN $p\bar{p}$ collider[72] suggest $M_t > 40$ GeV, conforming with the theoretical lower limit. In near future $p\bar{p}$ data from the Tevatron and the upgraded CERN colliders are expected to probe the upper mass limit[73] of the t-quark mass. These results are expected to be available by mid-nineties. The CDF collaboration at the Tevatron and UA1 and UA2 at CERN have put the experimental limit on top quark mass above or at least 60 GeV.[74] We shall confine our discussions here to the range $30 \leq M_t \leq 70$ GeV.

Table 2.6 gives some predicted toponium levels for different values of top quark mass. For $M(t\bar{t}) \sim 80$ GeV, we expect about 10 S-states below the threshold. A graph of the variation of the binding energies versus the mass of t-quark is shown in Fig.2.4 and its nature is found to be almost linear. The levels

Table 2.6. Energy levels of $t\bar{t}$ states.

Mass of t quark (GeV)	Energy levels for various states in GeV			
	1S	2S	1P	2P
30	59.15	59.78	59.64	60.02
35	69.07	69.71	69.58	69.97
40	79.01	79.66	79.53	79.92
45	88.95	89.60	89.49	89.87
50	98.89	99.56	99.45	99.84
55	108.84	109.51	109.41	109.80
60	118.78	119.48	119.38	119.77
65	128.73	129.44	129.35	129.74
70	138.68	139.40	139.32	139.71

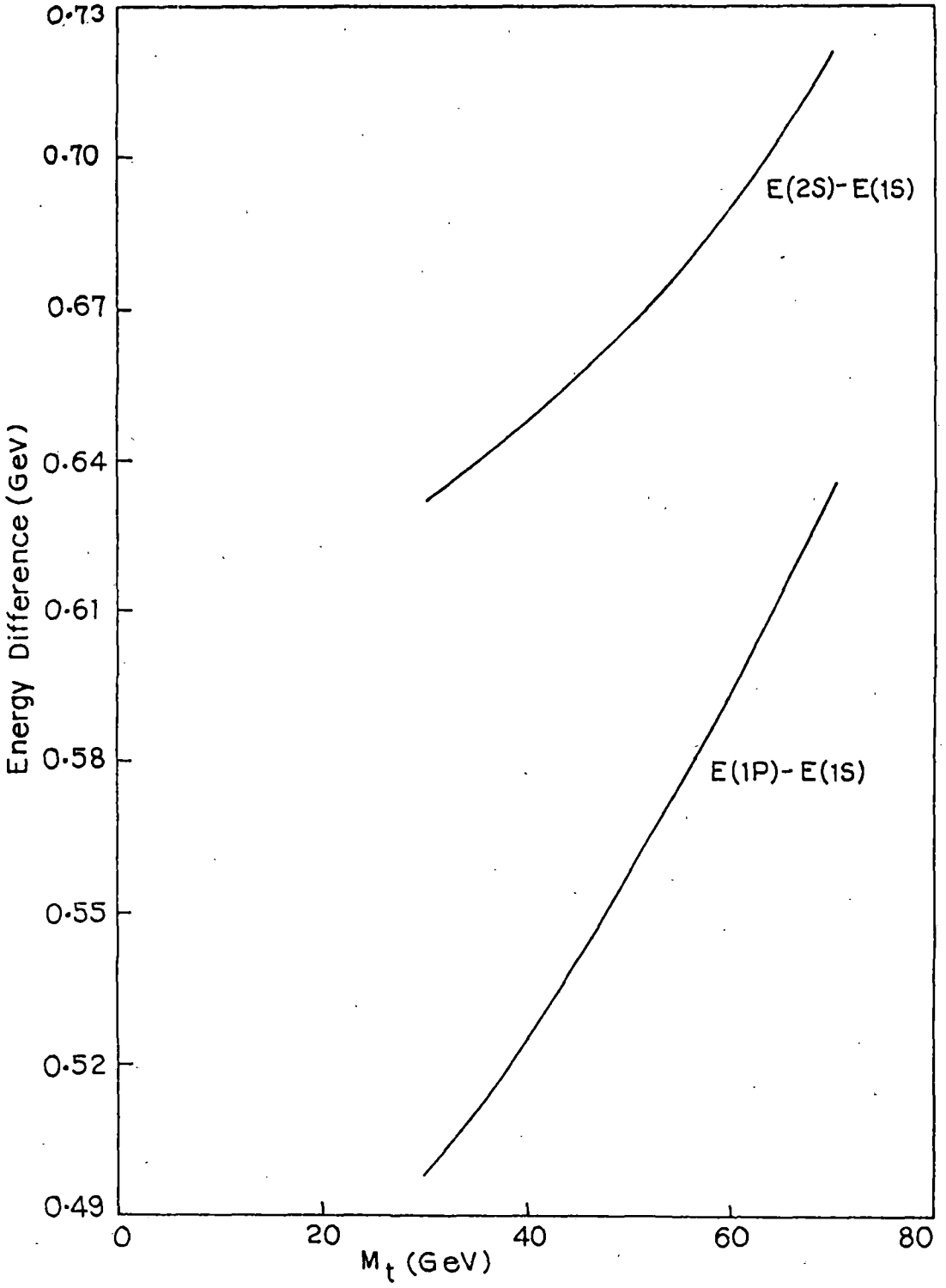

Fig. 2.4. Level Separation VS. top quark mass.

are not yet coulombic.

II.4. Total and hadronic decay widths of χ_b^J states :

The Crystal Ball Collaboration at DESY[19] have studied radiative decays of the Y(2S) resonance in which they detected two monochromatic photon lines at energies (107.0 ± 1.1 ± 1.3) MeV and (131.7 ± 0.9 ± 1.3) MeV along with a pair of leptons. The decay mechanism may be written as

$$\begin{aligned} Y(2S) &\rightarrow \gamma + \chi_b \\ &\qquad \hookrightarrow \gamma + Y(1S) \\ &\qquad\qquad \hookrightarrow e^+e^- \text{ or } \mu^+\mu^- \ . \end{aligned} \tag{2.6}$$

The product branching ratio is given by

$$\begin{aligned} BR_J\ [\ Y(2S) \rightarrow \gamma\gamma l^+l^-\ ] \equiv BR\ [\ Y(2S) \rightarrow \gamma\chi_b^J\ ] \times BR\ [\ \chi_b^J \rightarrow \gamma Y(1S)\ ] \\ \times BR\ [\ Y(1S) \rightarrow l^+l^-\ ] \end{aligned} \tag{2.7}$$

By making use of the experimental branching ratio, we can find out the total width and hadronic decay width of χ_b^J state, which is given by

$$\Gamma_{had}(\chi_b^J) = \Gamma_\gamma(\chi_b^J) \times \left[\frac{1}{BR\left(\chi_b^J \rightarrow \gamma\ Y(S)\right)} - 1 \right] . \tag{2.8}$$

Our calculated results are as follows :

(1) Calculated E1 transition widths :

Transition	Transition width in KeV
$1^3P_1 \rightarrow 1^3S_1$	35.034
$1^3P_2 \rightarrow 1^3S_1$	40.357
$2^3S_1 \rightarrow 1^3P_1$	2.000
$2^3S_1 \rightarrow 1^3P_2$	1.966

(2) We make use of the experimental values of the branching ratios[18]

$$BR_2 [\ \Upsilon(2S) \rightarrow \gamma\chi_b^2\ ] = (\ 5.8 \pm 0.7 \pm 1.0\ )\%$$

$$BR_1 [\ \Upsilon(2S) \rightarrow \gamma\chi_b^1\ ] = (\ 6.5 \pm 0.7 \pm 1.2\ )\%$$

to determine roughly the average total width of $\Upsilon(2S)$ ~ 33 KeV, which may be compared with the experimental results (44 ± 9) KeV.

(3) We next consider the χ_b^J states : From (2) above and the measured values of the product branching ratio $BR_2[\Upsilon(2S) \rightarrow \gamma\gamma l^+l^-] = (\ 4.4 \pm 0.9 \pm 0.5\ ) \times 10^{-4}$ and $BR_1[\Upsilon(2S) \rightarrow \gamma\gamma l^+l^-] = (\ 5.8 \pm 0.9 \pm 0.7\ ) \times 10^{-4}$, given by Crystal Ball Collaboration[19] and average branching ratio for $\Upsilon(1S) \rightarrow l^+l^-$ ~ 0.027,[28] we get the total width and the hadronic width of χ_b^J:

	Total width (KeV)	Hadronic width (KeV)
χ_b^2	143.63	103.27
χ_b^1	106.01	70.98

Since there is no measured value of the product branching ratio for χ_b^0 , we cannot determine its width, even if we have the E1

transition rates involving the χ_b^0 state. The experimental results involving χ_b^0 will be very much welcome.

II.5. Conclusions :

We have shown that the non-relativistic description of the heavy quarkonia by a potential comprising of a short-range QCD potential which is matched to a confining potential generates the mass spectrum and decay widths of the $b\bar{b}$ as well as $c\bar{c}$ states. We find that the values of the leptonic widths including Poggio-Schnitzer corrections are in good agreement with experiments in the case of $c\bar{c}$ states. However, this correction is negligible for heavy quarkonia. We are unable to find a good fit of E1 transition rates of $c\bar{c}$ due to the fact that we neglected the relativistic as well as coupled channel effects, which reduce the overlap between the two states considerably. It is expected that the parameters of the potential may require slight adjustment while calculating relativistic effects. Since the branching ratio of $b\bar{b}$ state has not been determined theoretically by us here, we use experimental branching ratio to determine the total width and hadronic width of the χ_b^1 and χ_b^2 states. The results show the overall efficacy of a non-relativistic description for the Heavy quarkonia. However, for quantitative agreement with experimental results, one should include spin-dependent interactions, which are relativistic in nature. This will be taken up in the next chapter.

* *CHAPTER III*

FINE-HYPERFINE INTERACTION

* A part of the contents of this chapter has already been published in Ref.(75).

III.1. Introduction :

The spin-averaged properties of heavy quarkonia seem to be described fairly accurately by a Schrödinger equation with a quark-antiquark potential, which has been determined empirically, with some guidance from quantum chromodynamics. The spin-independent potential is determined accurately at least in the range 0.1 fm < r <1 fm. The potential is in general agreement with the calculation of lattice gauge theory. The situation is, however, less satisfactory when one considers the spin-dependent effects, *e.g.* fine-hyperfine splittings. The fine-structures of χ-states, which have been measured fairly accurately presents, in particular, a case where the simple-minded theoretical results seem to fail. This may appear a bit surprising, since the fine-hyperfine interactions are essentially short-distance effects and one may expect a QCD-motivated potential to yield good results. However, fine-hyperfine interactions are relativistic in origin and the failure of the standard non-relativistic potentials may be due to the fact that the spin-dependent potentials are not related to the non-relativistic potentials in the simple way normally assumed. The method of studying the spin-dependent interactions have been developed by Eichten and Feinberg,[41] Buchmüller,[44,76] Gromes[35,42] and others.[8,39,46,48,49,77] Their prescription will be summarized in the next section. The Breit-Fermi interaction potential which is obtained within the

framework of Bethe-Salpeter equation are also discussed. In section III.3, we consider a modification of the Breit-Fermi interaction potential which leads to a better agreement with the experimental results. The calculated results are given in section III.4. Theoretical results obtained by some other authors have been compared with our results in this section. The possible modification of the results due to the inclusion of a pseudoscalar exchange potential is also studied. Our conclusions are summarized in the last section.

III.2. Breit-Fermi potential :

The general form of the nearly non-relativistic $Q\bar{Q}$ potential, as defined by the Wilson loop, can be written to lowest order in $(v/c)^2$ as

$$V(r) = V_{SI}(r) + \frac{S.L}{2M_Q^2}\left(-\frac{dV_{SI}}{rdr} + \frac{4}{r}\frac{dV_2(r)}{dr}\right) + \frac{1}{3M_Q^2}S_{12}V_3(r) + \frac{2}{3M_Q^2}S_1.S_2\,V_4(r)\,, \qquad (3.1)$$

where

$$S = S_1 + S_2 \quad \text{and} \quad S_{12} = \left(3(S_1.\hat{r})(S_2.\hat{r}) - S_1.S_2\right) \qquad (3.2)$$

and V_{SI} is the spin-independent potential, and V_2, V_3, V_4 are the spin-dependent ones, related to the correlation functions of colour electric and colour magnetic fields which are different from those that determine the spin-independent potential. The potentials V_2, V_3, V_4 may not, in principle, be simply related to

V_{SI}. However, it has been noted that a conceptually simple picture may be obtained if one assumes relations similar to those that emerge when one considers the Breit-Fermi interaction potentials obtained in the non-relativistic limit of a Bethe-Salpeter equation with vector and scalar exchange kernels. Thus one makes the following identification :

$$V_{SI}(r) \simeq V_{nR}(r) = V_v(r) + V_s(r) \tag{3.3}$$

$$V_2(r) = V_v(r) \tag{3.4}$$

$$V_3(r) = -\frac{d^2V_v(r)}{dr^2} + \frac{dV_v(r)/dr}{r} \tag{3.5}$$

$$V_4(r) = \nabla^2 V_v(r) \quad , \tag{3.6}$$

where $V_v(r)$ and $V_s(r)$ represent the vector and scalar exchange potentials respectively. With the usual non-relativistic reduction of the Bethe-Salpeter equation, the fine-hyperfine energies are given by

$$\langle V_{SD}(r) \rangle = a \langle L.S \rangle + b \langle S_{12} \rangle + c \langle S_1.S_2 \rangle \ ,$$

where,

$$a = \frac{1}{2M_Q^2} \left\langle \frac{3dV_v/dr - dV_s/dr}{r} \right\rangle \tag{3.7}$$

$$b = \frac{1}{3M_Q^2} \left\langle \frac{dV_v/dr}{r} - \frac{d^2V_v}{dr^2} \right\rangle \tag{3.8}$$

$$c = \frac{2}{3M_Q^2} \langle \nabla^2 V_v \rangle \qquad (3.9)$$

and $\langle S_1.S_2 \rangle = \frac{1}{2} [\, S(S+1) - \frac{3}{2} \,]$

$$\langle L.S \rangle = \frac{1}{2} [\, J(J+1) - L(L+1) - S(S+1) \,]$$

$$\langle S_{12} \rangle = \frac{-\langle L.S \rangle^2 - (1/2)\langle L.S \rangle + (1/3)\langle L^2 \rangle \langle S^2 \rangle}{(2L+3)(2L-1)} \,.$$

It can be seen that both scalar and vector potentials enter into the spin-orbit interaction term whereas the spin-spin and tensor interactions depend only on the vector part. The spin-dependent mass-splitting formula can be written conveniently in the matrix form as

(i)
$$\begin{vmatrix} M(^3S_1) \\ M(^1S_0) \end{vmatrix} = \begin{vmatrix} 1 & 1/4 \\ 1 & -3/4 \end{vmatrix} \begin{vmatrix} M_0(nS) \\ c(nS) \end{vmatrix} \quad \text{for S-states}$$

(ii)
$$\begin{vmatrix} M(^3P_2) \\ M(^3P_1) \\ M(^3P_0) \\ M(^1P_1) \end{vmatrix} = \begin{vmatrix} 1 & 1 & -1/10 & 1/4 \\ 1 & -1 & 1/2 & 1/4 \\ 1 & -2 & -1 & 1/4 \\ 1 & 0 & 0 & -3/4 \end{vmatrix} \begin{vmatrix} M_0(nP) \\ a(nP) \\ b(nP) \\ c(nP) \end{vmatrix} \quad \text{for P-states}$$

(iii)
$$\begin{vmatrix} M(^3D_3) \\ M(^3D_2) \\ M(^3D_1) \\ M(^1D_2) \end{vmatrix} = \begin{vmatrix} 1 & 2 & -1/7 & 1/4 \\ 1 & -1 & 1/2 & 1/4 \\ 1 & -3 & -1/2 & 1/4 \\ 1 & 0 & 0 & -3/4 \end{vmatrix} \begin{vmatrix} M_0(nD) \\ a(nD) \\ b(nD) \\ c(nD) \end{vmatrix} \quad \text{for D-states}$$

Here $M_0(nL)$ represents the spin-averaged mass of the system. Thus for P-states, the centre of gravity of the triplet state is given by

$$M.\,(\,^3P_{COG}\,) = [\,M(^3P_0) + 3\,M(^3P_1) + 5\,M(^3P_2)\,]\,/\,9\,.$$

From the known masses of ^3P_J states of $b\bar{b}$ and $c\bar{c}$ systems, it is customary to define the fine-structure ratio r as

$$r = \frac{(M_2 - M_1)}{(M_1 - M_0)} \qquad (3.10)$$

where M_J are the masses of the χ-states with total spin J. The experimental values give $r < 0.8$ for all χ-states. In the limit of a coulomb potential, $r = 0.8$. Experimentally $r = 0.67 \pm 0.05$ for $b\bar{b}(1P)$ and $r = 0.48 \pm 0.01$ for $c\bar{c}(1P)$. Therefore, as expected, the $b\bar{b}$ system is more coulombic in nature than $c\bar{c}$ system.

The simple prescription, Eqs. (3.3)-(3.6), however, imposes severe constraints on the potentials $V_{nR}(r)$ and $V_v(r)$ and it is not surprising that the potentials fail to account for the observed fine-hyperfine splittings. It is now recognised that the hyperfine structure of P-states, in particular, cannot be explained[78] within the framework mentioned above. Igi and Ono[50,79] have considered the radiative corrections to the potential, as given by Gupta, Radford and Repko[48,49] for the spin-dependent interactions and found that the recent data on h_b and h_c cannot be accounted for. Pantaleone and Tye,[47,80] using the potentials

derived by the method of Eichten and Feinberg,[41] have also reached similar conclusions. They even suggested a reexamination of the experimental results. Gupta *et al.*[81] have also noted that both $b\bar{b}$ and $c\bar{c}$ data cannot be fitted with the same set of potential parameters. It appears that the spin-dependent interactions are not yet understood and further investigation is essential.

III.3. Modified Breit-Fermi potential :

While looking for a modification, it will be useful to work within the framework of Breit-Fermi form, although the validity of the Eqs. (3.3) - (3.6), in particular, will have to be examined critically. We intend to undertake such a study. As a first step, we consider a simple empirical variation of the relations (3.3)-(3.6), aimed at fitting the fine-hyperfine data, without losing contact with the fairly successful non-relativistic treatment.

We note that while the static potential has to be equal to the sum of V_v and V_s (Gromes[35,42] sum rule), V_2 does not have to be equal to V_v. This provides a possible direction for introducing a modification. We write the non-relativistic $Q\bar{Q}$ potential as in the previous chapter, *e.g.*,

$$V_{nR} = f(r)V_{QCD}^{(2)}(r) + \left(1-f(r)\right)V_L(r)$$

where

$$f(r) = \frac{(1 + e^{-r_0/s})}{(1 + e^{(r-r_0)/s})} \quad ,$$

and $V^{(2)}_{QCD}(r)$ is the 2-loop QCD potential. The long-range part V_L is not well-determined and we choose

$$V_L(r) = Ar + B\,(1 + \ln\Lambda_{\overline{MS}}\, r) \quad . \tag{3.11}$$

The motivation for including the $\ln\Lambda_{\overline{MS}}\, r$ term may be mentioned here. As has been pointed out by Olsson and Suchyta,[82] the spin-orbit contribution of the confinement potential can be separated in the observed fine-structure of 1P states and the results are

$$\begin{aligned} \alpha_{conf}\,(b\bar{b}) &= -7.7 \pm 2.1 \text{ MeV} \\ \alpha_{conf}\,(c\bar{c}) &= -25.9 \pm 1.3 \text{ MeV} \quad , \end{aligned} \tag{3.12}$$

while a linear confinement term kr, with $k \sim 0.2$ GeV^2 gives the values $\alpha_{conf}(b\bar{b}) = -2.8$ MeV and $\alpha_{conf}(c\bar{c}) = -18$ MeV. Thus if the Breit-Fermi form is accepted, a modification in the long-range potential is necessary, and this can be done conveniently in the intermediate range of r values. Olsson and Suchyta[83] considered a modification of the form $V_L(r) = Ar - \alpha/r$, which is supported by lattice gauge calculations.[84] Lüsher[85] also suggested a similar form from flux-tube considerations. We, however, prefer the form (3.11) because it leads to a milder behavior for the corresponding spin-orbit term at short-distances. We now look for a simple modification of the standard Breit-Fermi relations by choosing V_{nR}

$= V_2(r) + V_s(r)$, where

$$V_2(r) = f(r)V_{QCD}^{(2)}(r) - \Lambda_{\overline{MS}}^3 r^2(1-\beta/r), \qquad r \leq \beta$$

$$= 0 \qquad r > \beta \qquad (3.13)$$

$$V_s(r) = \left(1 - f(r)\right)V_L(r) + \Lambda_{\overline{MS}}^3 r^2(1-\beta/r), \qquad r \leq \beta$$

$$= \left(1 - f(r)\right)V_L(r) \qquad r > \beta \qquad (3.14)$$

$$V_3(r) = -d^2V_2(r)/dr^2 + \frac{dV_2(r)/dr}{r} \qquad (3.15)$$

$$V_4(r) = \nabla^2 V_2(r) \ . \qquad (3.16)$$

The potentials chosen have the following features :

(1) The non-relativistic potential V_{nR} remains unchanged. There is no discontinuity in V_{nR}, and the discontinuity in dV_{nR}/dr occurs at a large value of $r = \beta = 1.835$ fm, so that the short-range spin-dependent results are not appreciably disturbed.

(2) $V_2(r)$ differs from $V_v(r)$, the difference indicating a possible contribution from non-perturbative interactions. As $r \to 0$, one regains the one-gluon-exchange term.

(3) The Woods-Saxon function has been introduced[66] to interpolate between the perturbative and the confining regions. One may hope that the fine-hyperfine splittings could be fitted by adjusting these parameters. The expection, however, is not fulfilled. The

obvious conclusion is that within the framework of Breit-Fermi scheme, the potentials $V_v(r)$ and $V_L(r)$ need some modifications. We have given above a simple modification with an extra parameter β.

(4) At $r = \beta < \Lambda_{\overline{MS}}^{-1}$, $f(r)V_v(r)$ is already negligibly small, where a cut-off is introduced. The cut-off is needed anyway to eliminate the unphysical perturbative QCD singularity at $r = \Lambda_{\overline{MS}}^{-1}$. The cut-off should not affect the calculated results with our choice of $\Lambda_{\overline{MS}} = 196$ MeV.

(5) The potentials $V_2(r)$ and $V_s(r)$ and $V_t = V_{nR}$ have been shown in Fig.3.1. Whether the potential $V_2(r)$ should still be called the vector exchange potential is not clear, but the extensive modification of the QCD potentials needed even for a modest fit with the experimental fine-hyperfine results is an indication of the constraints on the potentials.

III.4. Fine-hyperfine splittings :

With the choice of V_{nR} as in above, we have solved the Schrödinger equation numerically and have also evaluted the quantities relevant for fine-hyperfine splitting replacing V_v by V_2 in Eqs. (3.7) - (3.9). The values of the parameters M_b, M_c, $\Lambda_{\overline{MS}}$, A, B, r_o and s are the same as in the previous chapter. To determine fine-hyperfine splittings, we have used only one extra parameter β =1.835 fm.

The results obtained may be summarized as follows :

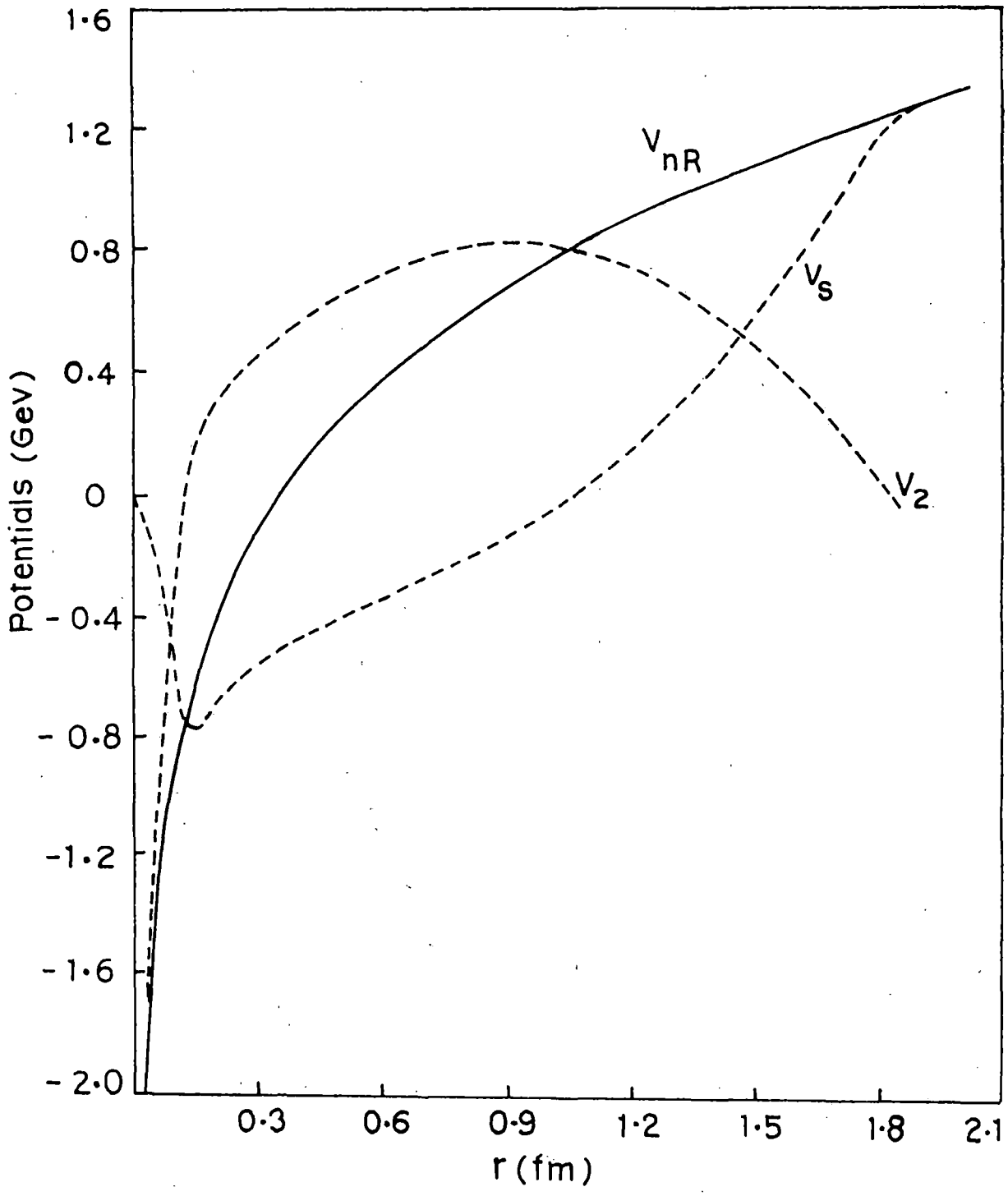

Fig.3.1. The $Q\bar{Q}$ potentials $V_2(r)$, $V_s(r)$ and the total potential $V_{nR} = V_2(r) + V_s(r)$.

(1) The non-relativistic potential V_{nR} gives the spin-averaged spectra fairly accurately, excepting for the centre of gravity mass for the 1P states, which is about 15 MeV less than the experimental value. In the case of Martin potential,[86] the lowest mass Y P-state is obtained 40 MeV below the COG value. The absence of a coulomb-like singularity raises the S-states with respect to P-states. This problem exists with Cornell potential also, although not recognized by the earlier workers. The reason, as given by Jacobs *et al.*,[87] is that earlier workers used the ψ, 1P, ψ' masses while one considers, in the present context, the COG values of the split levels. For ψ and ψ', this change means a difference of about 25-30 MeV, whereas the shift for 1P state is much smaller, leading to the observed disagreement. We have not tried to remedy this, because the fine-hyperfine splittings are not likely to be much altered by this small shift of the COG value. We have not considered the spin-independent relativistic corrections. For the $b\bar{b}$ states, these are anyway very small.

(2) To study the spin-dependent interactions, we first consider the Breit-Fermi potentials without any modification, *viz.* $V_2 = V_v$ and $V_s = \left(1-f(r)\right) V_L$. The calculated values for a,b,c for the five levels (1S,2S,1P of $c\bar{c}$ and 1P,2P of $b\bar{b}$), for which the experimental results are available, have been shown in Table 3.1. It is obvious that the naive choice $V_2 = V_v$ and $V_s = \left(1-f(r)\right) V_L$ do not agree at all with the experimental results. Note, in particular, that with $V_2 = V_v$, one gets negative values for a and c

Table 3.1. Results for unmodified Breit-Fermi interaction (i) without and (ii) with pseudoscalar exchange contribution.

State	a(MeV)		b(MeV)		c(MeV)	
	Expt.	Theory	Expt.	Theory	Expt.	Theory
$b\bar{b}$(1P)	14.1 ± 0.4	5.64	12.0 ± 0.9	(i) 9.44 (ii)12.16	5.4 ± 2.2	(i)-4.87 (ii)-5.12
$b\bar{b}$(2P)	10.3 ± 1.2	6.97	9.8 ± 1.4	(i) 7.67 (ii)13.54		(i)-3.16 (ii)-0.35
$c\bar{c}$(1S)					116 ± 5	(i)32.37[a] (ii)167.82[a]
$c\bar{c}$(2S)					92 ± 5	(i)26.04[a] (ii)145.65[a]
$c\bar{c}$(1P)	34.9 ± 0.3	-18.41	40.1 ± 0.8	(i) 8.64 (ii)30.18	0 ± 0.9	(i) -5.99 (ii)-1.25

[a]No $\delta^3(r)$ term was considered for evaluating c.

for $c\bar{c}$ states, while the experimental values are positive. A modification of the naive choice is definitely called for.

(3) With the choice of Eqs.(3.13)-(3.16), we get the results shown in Table 3.2. The overall agreement for the fine-hyperfine splittings of the P-states for both $b\bar{b}$ and $c\bar{c}$ systems is satisfactory, but leaves scopes for improvement. It has been possible to get a positive value (though smaller than the experimental value) for c for Y(1P) state. This may be taken as indicative of the trend of the modification needed to explain these data. The fine interaction results are in general agreement with the experimental results. It may be pointed out that our attempt to get a positive c for 1P $b\bar{b}$ state has led to a little worsening of the agreement for the values of a and b. This can be seen by increasing the value of β a little, say to β = 1.86 fm where we get a = 19.33 MeV, b = 12.9 MeV and c = 1.94 MeV for $b\bar{b}$ 1P state. While smaller values of a and b can be obtained by choosing a smaller β, the value for c becomes negative. Igi and Ono[79] and Pantaleone and Tye[80] obtained negative values for c. None of the calculations could accurately fit the value of b for the 1P($c\bar{c}$) state. Also, the value of c(2S) is generally lower than the experimental results. We have not considered any $\delta^3(r)$ term in the spin-spin potential. Our values for a are slightly higher than the experimental results. It is possible that the $\ln\Lambda_{\overline{MS}}\, r$ term in the confining potential cannot describe accurately the necessary modification in the potential in the distance scales scanned by 1P or 2P $b\bar{b}$ states.

Table 3.2. Expectation values of the spin-orbit (a), tensor (b) and spin-spin (c) potentials obtained in different models.

State	Values of	Experimental values in MeV	Pantaleone *et al.*[47,80] (MeV)	Igi and Ono[50,79] with $\Lambda_{\overline{MS}}$ = 200 MeV (MeV)	Ours Eqs. (3.13) -(3.16) (MeV)
$b\bar{b}(1S)$	c		35.0	39.5	58.83[b]
$b\bar{b}(2S)$	c		19.0	21.5	30.8[b]
	a	14.1 ± 0.4	13.0	14.3	19.07
$b\bar{b}(1P)$	b	12.0 ± 0.9	9.0	11.76	12.86[b]
	c	5.4 ± 2.2	-0.4,-0.5[a]	-0.772	1.74
	a	10.3 ± 1.2	9.3	9.38	13.88
$b\bar{b}(2P)$	b	9.8 ± 1.4	6.7	7.92	9.98
	c		-0.3,-0.4[a]	-0.542	-0.88
$c\bar{c}(1S)$	c	116 ± 5	101.0	140	122.69[b]
$c\bar{c}(2S)$	c	92 ± 5	69.0	84	34.78[b]
	a	34.9 ± 0.3	48.0	40.5	33.22
$c\bar{c}(1P)$	b	40.1 ± 0.8	46.0	43.6	30.97
	c	0 ± 0.9	-3.6,-1.4[a]	-3.49	0.98

[a] New values obtained.[80]

[b] No $\delta^3(r)$ term considered for evaluating c.

(4) Table 3.3 and Table 3.4 show the fine-hyperfine structure of $b\bar{b}$ and $c\bar{c}$ systems. We have compared our results with recent calculations by Gupta, Radford and Suchyta III[88] (GRS), Schmitz, Beavis and Kaus[89] (SBK), Fulcher[51] (FUL) and also the experimental values[28]. However, GRS use a non-singular potential by considering different values of the scalar-vector mixing parameter for different flavours which need a justification. The potential chosen by SBK includes a running coupling constant $\alpha(r)$ with some modification to avoid a singularity. Fulcher's work is based on a one-loop perturbative potential supplemented by a linear confining potential and a long-range spin-orbit potential. The pseudoscalar partner η_c of ψ meson in our case is very close to the experimental value whereas the $^1S_0$ partner of $\psi'(\eta_c')$ is too high. In the Y system, the predicted centre of gravity value of 1P state is too low if we fix the value of 1^3S_1 energy level at 9460 MeV. SBK also found similar differences but the results of FUL agree with the experiments. However, our result for the COG of 2P states is very close to the experimental value and it almost agrees with FUL's result whereas in SBK's calculation, the COG is shifted upward by approximately 20 MeV. In case of ψ mesons, the spin-averaged χ-level predicted by us is about 20 MeV below its observed value. The energy levels of D-state of $b\bar{b}$ and $c\bar{c}$ systems are listed in Table 3.5. Here, our results are compared with the calculated results of FUL[51] and also of Sebastian *et al.*[90] (SGZ) who used the potential proposed by Gupta, Radford and Repko. In the Y system, almost all the potential models predict nearly the

Table 3.3. Energy level splittings for the Υ system.

State	Experimental value (MeV)	GRS[88] (MeV)	FUL[51] (MeV)	SBK[89] (MeV)	OURS (MeV)
$1^3S_1(\Upsilon)$	9460.32 ± 0.22	9460.0	9460	9461	9460.21
$1^1S_0(\eta_b)$		9412.2	9420		9401.38
$2^3S_1(\Upsilon')$	10023.29 ± 0.31	10015.8	10006	10023	10037.70
$2^1S_0(\eta_b')$		9992.5	9983		10006.90
$3^3S_1(\Upsilon'')$	10355.3 ± 0.5	10357.8	10355		10362.95
$3^1S_0(\eta_b'')$		10339.7	10336		10343.14
$4^3S_1(\Upsilon''')$	10580 ± 3.5				10596.51
$4^1S_0(\eta_b''')$					10582.46
$1^3P_2(\chi_b^2)$	9913.2 ± 0.6	9913.9	9908	9908	9904.02
$1^3P_1(\chi_b^1)$	9891.9 ± 0.7	9893.3	9895	9880	9873.60
$1^3P_0(\chi_b^0)$	9859.8 ± 1.3	9861.8	9874	9849	9835.24
$1^1P_1(h_b)$	9894.8 ± 1.5	9900.1	9901		9884.50
$2^3P_2(\chi_b'^2)$	10269.0 ± 0.7	10269.8	10268	10292	10269.66
$2^3P_1(\chi_b'^1)$	10255.2 ± 0.4	10253.7	10256	10270	10247.89
$2^3P_0(\chi_b'^0)$	10235.3 ± 1.1	10228.8	10239	10245	10219.04
$2^1P_1(h_b')$		10259.0	10262		10257.66

Table 3.4 Energy level splittings for the ψ system.

State	Experimental value (MeV)	GRS[88] (MeV)	SBK[89] (MeV)	OURS (MeV)
$1^3S_1(\psi)$	3096.93 ± 0.09	3096.9	3107	3099.37
$1^1S_0(\eta_c)$	2979.6 $^{+1.7}_{-1.6}$	2981.1	2982	2976.68
$2^3S_1(\psi')$	3686.0 ± 0.1	3689.7	3692	3671.50
$2^1S_0(\eta_c')$	3594.0 ± 5.0	3619.1		3636.72
$1^3P_2(\chi_c^2)$	3556.3 ± 0.4	3553.5	3561	3535.57
$1^3P_1(\chi_c^1)$	3510.6 ± 0.5	3507.0	3490	3487.71
$1^3P_0(\chi_c^0)$	3415.1 ± 1.0	3412.2	3412	3408.04
$1^1P_1(h_c)$	3525.4 ± 0.8[a]	3518.5		3504.47

[a]Baglin et al. (Ref.27).

Table 3.5. Predicted D-state energy level splittings for Y and ψ systems in MeV.

State	$b\bar{b}$ system			$c\bar{c}$ system	
	FUL[51]	SGZ[90]	OURS	SGZ[90]	OURS
1^3D_3	10162	10153	10163.3	3830	3783.9
1^3D_2	10160	10149	10152.4	3822	3782.6
1^3D_1	10155	10143	10141.5	3801	3782.1
1^1D_2	10160	10150	10153.8	3822	3800.0
2^3D_3		10451	10436.6		
2^3D_2		10446	10432.0		
2^3D_1		10440	10425.2		
2^1D_2		10447	10433.6		

same spin-averaged D-state B.E. to within ± 10 MeV. For the 1D level of $c\bar{c}$, the experimental value of 1^3D_1 state is already known, i.e. $M(^3D_1)$ = 3769.9 ± 2.5 MeV. From the Table 3.5, we see that our results are marginally better than SGZ's results, but leaves scope for improvement. Moreover, using the theoretical value of the radiated photon energy, we have studied the E1 transition rates for both $b\bar{b}$ and $c\bar{c}$ systems. These are listed in Table 3.6 and Table 3.7.

(5) While we are convinced of the need for a modification of the naive BF interaction potentials, the question whether this could come as a contribution from a possible pseudoscalar exchange potential[35,42] should also be examined. The pseudoscalar exchange makes no contribution in the non-relativistic limit but contributes the following $(v/c)^2$ correction to the fine-hyperfine interaction :

$$H_{PS} = \frac{1}{3M_Q^2} S_1 . S_2 \nabla^2 V_{PS}(r) + \frac{1}{3M_Q^2} \left(d^2V_{PS}/dr^2 - \frac{dV_{PS}/dr}{r} \right) S_{12} . \qquad (3.17)$$

We choose a fairly general $V_{PS}(r)$, i.e. ,

$$V_{PS}(r) = E/r + F \ln\Lambda_{\overline{MS}}\, r + Gr + Hr^2 \quad , \qquad (3.18)$$

and try for a fit with the experimental results for b and c. Note that r^2 term does not contribute to b and the $1/r$ term contributes only a $\delta^3(r)$ term to c, which we neglect for the time being. The results, as shown in Table 3.1 disagree with the experimental

Table 3.6. E1 transition rates for Y states.

Transition	Experimental ω (MeV)	Calculated ω (MeV)	Γ_{E1} (Expt.) (KeV)	Γ_{E1} (Theo.) (KeV)
$2^3S_1 \rightarrow 1^3P_0$	162.3 ± 1.3	200.42	1.29 ± 0.31	2.40
1^3P_1	130.7 ± 0.7	162.76	2.01 ± 0.49	3.86
1^3P_2	109.5 ± 0.6	132.79	1.98 ± 0.48	3.50
$3^3S_1 \rightarrow 1^3P_0$	483.8 ± 1.4	512.27		0.01
1^3P_1	453.2 ± 0.9	477.80	0.04 ± 0.03	0.03
1^3P_2	432.8 ± 0.8	448.77	0.06 ± 0.05	0.04
$3^3S_1 \rightarrow 2^3P_0$	119.3 ± 1.1	142.91	1.22 ± 0.3	2.54
2^3P_1	99.6 ± 0.4	114.42	3.08 ± 0.6	3.90
2^3P_2	85.9 ± 0.7	92.87	3.26 ± 0.7	3.48
$1^3P_0 \rightarrow 1^3S_1$	391.7 ± 1.3	367.88		23.13
1^3P_1	422.5 ± 0.7	404.73		30.80
1^3P_2	442.9 ± 0.6	433.87		37.94
$2^3P_0 \rightarrow 1^3S_1$	741.5 ± 2.3	730.66		6.45
2^3P_1	764.8 ± 0.8	757.41		7.19
2^3P_2	776.8 ± 0.7	777.55		7.78
$2^3P_0 \rightarrow 2^3S_1$	205.0 ± 2.3	179.73		8.35
2^3P_1	229.7 ± 0.9	208.03		12.95
2^3P_2	242.3 ± 0.8	229.34		17.35

Table 3.7. E1 transition rates for ψ states.

Transition	Experimental ω (MeV)	Calculated ω (MeV)	Γ_{E1} (Theo.) (KeV)
$2^3S_1 \rightarrow 1^3P_0$	261.0	254.0	64.36
1^3P_1	171.8	179.19	67.79
1^3P_2	127.7	133.41	46.63
$1^3P_0 \rightarrow 1^3S_1$	303.2	294.69	170.08
1^3P_1	388.7	366.72	329.69
1^3P_2	429.4	409.29	458.35
$3^3S_1 \rightarrow 1^3P_0$		558.98	0.36
1^3P_1		490.52	0.72
1^3P_2		448.64	0.92
$3^3S_1 \rightarrow 2^3P_0$		149.55	37.48
2^3P_1		111.94	47.16
2^3P_2		118.48	93.20
$2^3P_0 \rightarrow 1^3S_1$		685.78	64.11
2^3P_1		717.64	73.47
2^3P_2		712.15	71.79
$2^3P_0 \rightarrow 2^3S_1$		184.01	124.50
2^3P_1		220.88	215.34
2^3P_2		214.52	197.27

results. The parameters have been chosen as E = 1.297, F = 3.2 GeV, G = -2.052 GeV^2 and H = 0.1636 GeV^3. We note, in particular, that (1) pseudoscalar exchange term does not modify the spin-orbit interaction and hence the value of a remains unacceptably low, (2) c for $b\bar{b}(1P)$ is still negative and (3) c for 1S and 2S states can be altered by including a term $k\delta^3(r)S_1.S_2$ with k = 0.073 GeV^{-2}, giving for the $c\bar{c}$ system, the values $c(1S)$ = 116 MeV and $c(2S)$ = 117.6 MeV, the latter being about 25 MeV larger than the experimental value. Our conclusion is that the addition of a pseudoscalar exchange potential alone is not sufficient.

III.5. Conclusions :

We have shown that the naive Breit-Fermi interactions (Eqs.3.3-3.6) are not consistent with the fine-hyperfine splittings of heavy quarkonia. The formal relationships may perhaps be maintained if the vector and scalar potentials are modified at least in the intermediate range of r values. The modification cannot be described by a pseudoscalar exchange potential. It appears that the measurement of the splittings of a few more levels should provide sufficient additional constraints and help in deciding if the Breit-Fermi form of interaction is at all valid for heavy quarkonia.

* CHAPTER IV

EXACT RESULTS FOR HYPERFINE INTERACTION

* A major part of the contents of this chapter has already been reported in Refs.(91) and (92).

IV.1. Introduction :

As pointed out in the earlier chapter, the spin-dependent potentials are not yet known accurately. The recently discovered hyperfine splitting of P-states cannot be accomodated comfortably within the framework of the standard Breit-Fermi form. The uncertainty regarding the long-range confining part of the potential is one of the factors contributing to the complexity of the problem. However, the S-states of the quarkonia have only hyperfine splitting and therefore, a careful study of η_b and η_c states can provide some useful information about the spin-dependent potential $V_4(r)$ and hence about $V_2(r)$, if Breit-Fermi form [Eqs.(3.1,3.3-3.6)] is accepted. It may be mentioned that the standard approach leads to highly singular terms, like $1/r^3$ and $\delta^3(r)$, for the hyperfine interactions. As has been pointed out by Bhaduri *et al.*,[93] a treatment of such singular potentials is not reliable as the hamiltonian becomes unbounded. The conventional approach has been to ignore this difficulty and treat the singular terms perturbatively. Some attempts have, of course, been made to recast the spin-dependent potentials in less singular form. Introducing an additional parameter, some authors[94] used a cut-off to reduce the singularity. Ono and Schöberl[95] replaced $\delta^3(r)$ by a short-ranged function and Gupta[96] obtained a form of the $Q\bar{Q}$ potential which is not more singular than $1/r^2$. Obviously, the problem needs further

investigation. Apart from the hyperfine splitting, the decay widths of the $^3S_1$ and $^1S_0$ states may provide some essential information. Some experimental results on these decay widths are already available. Model independent or exact results or bounds on the wave-functions at the origin, even if weak, will be very useful in this context. We present in this chapter some general results which are valid for a large class of $Q\bar{Q}$ potentials with a generally expected radial dependence.

The presentation in this chapter is as follows. In section IV.2, some inequalities for the wave-function at the origin, valid for a general class of $Q\bar{Q}$ potential have been obtained. In section IV.3, we make use of the $Q\bar{Q}$ potential obtained by Gupta which exhibits an explicit mass dependence and obtain some exact results for the hyperfine splittings of the S-states. These are used to obtain limits on the decay width of the η_b states. The final section gives our conclusions.

IV.2. Some inequalities for S-state wave-functions :

For a class of $Q\bar{Q}$ potentials, it is possible to prove the inequality,

$$\psi_s(0) > \psi_t(0) \quad , \tag{4.1}$$

where $\psi_t(r)$ and $\psi_s(r)$ denote the triplet and singlet radial wave-functions. We write $\psi_t(r) = u_t(r)/r$ and $\psi_s(r) = u_s(r)/r$ where $u_t(r)$ and $u_s(r)$, chosen real and positive, satisfy the

Schrödinger equations

$$\frac{d^2u_t}{dr^2} + \frac{2\mu}{\hbar^2}\left[E_t - V_0(r) - \frac{1}{4}V_\sigma(r)\right]u_t = 0 \qquad (4.2)$$

and

$$\frac{d^2u_s}{dr^2} + \frac{2\mu}{\hbar^2}\left[E_s - V_0(r) + \frac{3}{4}V_\sigma(r)\right]u_s = 0 \ . \qquad (4.3)$$

We assume that the spin-independent potential $V_0(r)$ is funnel-shaped with $dV_0/dr > 0$ and $d^2V_0/dr^2 < 0$ and that the hyperfine potential $V_\sigma(r)$ decreases monotonically, $dV_\sigma/dr < 0$. While the first assumption is generally accepted, the second is reasonable or at least there is no known objection against it. Note that $V_\sigma(r)$ is short-ranged and in the Breit-Fermi form, $V_\sigma = \nabla^2 V_v$, V_v being the vector exchange potential. We, however, ignore any $\delta^3(r)$ type term and assume that $V_\sigma(r)$ can be given in terms of a short-ranged continuous function.

To derive the inequality we follow the steps given in Ref. (97) which generalise the techniques developed by Grosse and Martin.[98] The steps are outlined below :

a) We know that at a large distance, there is no spin-spin interaction, $V_\sigma(r) \to 0$ as $r \to \infty$. From the large distance behavior of the Eqs. (4.2) and (4.3), we see that

$$u_t(r) > u_s(r) \quad \text{as} \quad r \to \infty \ , \ \text{since} \ E_t > E_s \ ,$$

as given by experimental results for both $b\bar{b}$ and $c\bar{c}$ states.

b) We note that the Wronskian

$$I(r) = \left(u_s \frac{du_t}{dr} - u_t \frac{du_s}{dr} \right)(r)$$

$$= \frac{2\mu}{\hbar^2} \int_0^r u_t u_s \left[V_\sigma(r) - (E_t - E_s) \right] dr \qquad (4.4)$$

is also given by

$$I(r) = - \frac{2\mu}{\hbar^2} \int_r^\infty u_t u_s \left[V_\sigma(r) - (E_t - E_s) \right] dr \qquad (4.5)$$

as $I(\infty) = 0$. Note that for $r \sim 0$, $I(r) > 0$ and for $r \to \infty$, $I(r) > 0$.

c) We note that since V_σ is monotonic, the integrand has only one zero, say at $r = r_o$. Hence for $r < r_o$, we use Eq. (4.4) and for $r > r_o$, we use Eq. (4.5) to show that $I(r) > 0$ for all r. One can now prove that $u_t - u_s$ has only one zero, say at $r = r_1$. From (4.4), we get

$$u_s(r_1) \left[u_t'(r_1) - u_s'(r_1) \right] > 0 ,$$

and since $u > 0$, we see that $u_t - u_s$ can vanish only once.

d) Since $u_t(r) > u_s(r)$ as $r \to \infty$ and $u_t - u_s$ vanishes only once, we see that $u_s > u_t$ near the origin.

e) We now consider the expression

$$|\psi_t(0)|^2 - |\psi_s(0)|^2 = \int_0^\infty (u_t^2 - u_s^2) \frac{dV_o}{dr} dr + \frac{1}{4} \int_0^\infty (3u_s^2 + u_t^2) \frac{dV_\sigma}{dr} dr$$

$$< \int_0^\infty (u_t^2 - u_s^2) \frac{dV_o}{dr} dr \quad , \quad \text{since} \quad \frac{dV_o}{dr} < 0 \ .$$

Since both u_t and u_s are normalised , we have

$$|\psi_t(0)|^2 - |\psi_s(0)|^2 < \int_0^\infty (u_t^2 - u_s^2) \left[\frac{dV_o}{dr} - \frac{dV_o}{dr}|_{r=r_1} \right] dr$$

$$< 0 \ , \quad \text{since} \quad \frac{d^2V_o}{dr^2} < 0 \ . \qquad (4.6)$$

Thus the singlet wave-function is larger than the triplet wave-function at the origin, although in perturbative calculations, one takes $\psi_t(r) = \psi_s(r)$.

The inequality (4.6) may be converted into useful inequalities for the decay widths of the η_b and η_c states. We first note some useful QCD relations involving wave-functions at the origin of the vector meson v :

$$\Gamma(v \to \mu^+\mu^-) = \frac{16\pi}{M_v^2} e_Q^2 \alpha^2 |\psi_t(0)|^2 \ , \qquad (4.7)$$

$$\Gamma(v \to 3g) = \frac{160}{81M_v^2} \alpha_s^3 (\pi^2 - 9) |\psi_t(0)|^2 \ , \qquad (4.8)$$

$$\Gamma(v \to 2g\gamma) = \frac{128}{9} \alpha \frac{e_Q^2}{M_v^2} \alpha_s^2 (\pi^2 - 9) |\psi_t(0)|^2 \ , \qquad (4.9)$$

$$\Gamma(\eta_Q \to 2g) = \frac{32\pi}{3M^2(\eta_Q)} \alpha_s^2 |\psi_s(0)|^2 \ . \qquad (4.10)$$

Using experimental values[28] for $\Gamma(\psi \to 3g) = 58.5$ KeV and $\Gamma(\eta_c \to 2g) = 10.3^{+3.8}_{-3.4}$ MeV, we get from Eqs. (4.8) and (4.10),

$$\frac{|\psi_t(0)|^2}{|\psi_s(0)|^2} = 0.541^{-0.146}_{+0.267} \qquad (4.11)$$

if $\alpha_s(c\bar{c}) = 0.2048$, which may be obtained by considering the ratio of (4.8) and (4.7) and using the experimental value for $\Gamma_\psi(e^+e^-) = 4.72 \pm 0.35$ KeV. Thus experimentally $\psi_t(0)/\psi_s(0) \approx 0.6 - 0.9$ for the $c\bar{c}$ system. In case of $b\bar{b}$ system, using the input value of $\Gamma(\Upsilon \to e^+e^-) = 1.34 \pm 0.05$ KeV, we get from Eq. (4.7), the value of $|\psi_t(0)|^2_{b\bar{b}} = 0.403$ GeV^3, which now becomes a lower bound for the wave-function at the origin of the yet unobserved $^1S_0$ $b\bar{b}$ state. The simple inequality (4.6) should hold for all S-states for all heavy quarkonia for the class of potentials considered and hence useful in predicting the order of the two-gluon widths for all η_Q states, yet to be discovered.

IV.3. Mass-dependent potential and decay width of η_b :

As pointed out earlier, most of the existing potential models involve highly singular interaction terms, like $\delta^3(r)$ or $1/r^3$ terms. The validity of a perturbative calculation with such terms is indeed questionable. Gupta[96] has proposed a new $Q\bar{Q}$ potential, which is less singular. This is obtained by considering a non-relativistic approximation of the $Q\bar{Q}$ scattering matrix

element by treating p^2/p_o^2 (rather than p^2/M^2) as the small expansion parameter, where $p^2 = \frac{1}{4}K^2 + \frac{1}{4}S^2$, $K = p' - p$, $S = p' + p$, it being assumed that S^2 is very small compared to K^2. The approximation leads to the second-order perturbative potential

$$V(r) = -\frac{4\alpha_s}{3}\left[\frac{1}{r} - \frac{4e^{-2Mr}}{3r}\left(S^2 - \frac{3}{4}\right) - \frac{3f_1}{2r}L.S - \frac{f_2}{4r}S_{12}\right] + Ar, \quad (4.12)$$

where

$$f_1 = \left[1 - \left(1 + 2Mr\right)e^{-2Mr}\right] / M^2r^2 , \quad (4.13)$$

$$f_2 = \left[1 - \left(1 + 2Mr + \frac{4}{3}M^2r^2\right)e^{-2Mr}\right] / M^2r^2 . \quad (4.14)$$

The potential has some interesting features, the most notable being its explicit mass dependence. We note that for an S-state, the potential may be written as

$$V(r) = M\phi_1(Mr) + Ar , \quad (4.15)$$

where $\phi_1(Mr)$ is a matrix function of Mr. In a recent paper, Gupta *et al.*[88] have taken a mixture of scalar and vector exchange terms with an arbitrary mixing parameter B and have chosen different values of B for the $b\bar{b}$ and $c\bar{c}$ systems. A justification for this choice is not clear. If we assume that B is the same for all flavours and that the $Q\bar{Q}$ potential is, in fact, of the type (4.15), we may use the mass scaling properties of the corresponding Schrödinger equation to derive some interesting results.

Let M_c, M_b be the quark masses and let $\phi_s^c(r) = \frac{u(r)}{r}$ and $\phi_s^b(r) = \frac{v(r)}{r}$ be the singlet radial wave-functions satisfying

$$\frac{d^2u}{dr^2} + \frac{2M_c}{\hbar^2}\left[E - M_c\phi(M_c r) - Ar \right]u = 0 \qquad (4.16)$$

$$\frac{d^2v}{dr^2} + \frac{2M_b}{\hbar^2}\left[E' - M_b\phi(M_b r) - Ar \right]v = 0 \ . \qquad (4.17)$$

We now consider a scaling transformation, $r' = \frac{M_b}{M_c} r$, of Eq. (4.17) and substitute $\omega(r) = \left(\frac{M_b}{M_c} \right)^{1/2} v(r)$. Arguments similar to those given before, will lead to the inequality

$$\left(\frac{M_b}{M_c} \right)^3 |\phi_s^c(0)|^2 > |\phi_s^b(0)|^2 \ . \qquad (4.18)$$

This behaviour is, in fact, expected even in more general cases. For a mass-independent power-law potential $V = \lambda r^\nu$, one gets

$$|\psi_M(0)|^2 \propto (M\lambda)^{3/(2+\nu)} \ . \qquad (4.19)$$

Thus for a coulomb potential ($\nu = -1$), $|\psi_M(0)|^2/M^3$ is a constant, but for $\nu > -1$, $|\psi_M(0)|^2/M^3$ decreases as M increases as in the case of Gupta's[96] potential. For $-2 < \nu < -1$, the ratio increases with M. The inequality (4.18) is a weak one but can still be converted into useful results, as is shown below:

a) We note that with $M_b = 4.78$ GeV and $M_c = 1.36$ GeV, which we have used in the previous chapter to fit the fine-hyperfine

spectra, the inequality gives

$$|\phi_s^c(0)|^2 \;>\; 0.023\;|\phi_s^b(0)|^2 \quad . \tag{4.20}$$

b) Using (4.10) and the experimental value of $M(\eta_c) = 2979.6^{+1.7}_{-1.6}$ MeV, we get $|\phi_s^c(0)|^2 = 0.0651$ GeV^3. Thus the upper bound of $|\phi_s^b(0)|^2$ is $\sim$ 2.83 GeV^3.

c) One may estimate $\alpha_s(b\bar{b})$ from the ratio[99]

$$\frac{\Gamma(\,\Upsilon(1S) \to 2g\gamma\,)}{\Gamma(\,\Upsilon(1S) \to 3g\,)} = \frac{36}{5}\,\frac{\alpha}{\alpha_s(b\bar{b})}\,e_Q^2 \;\approx\; \frac{3}{100} \tag{4.21}$$

giving $\alpha_s(b\bar{b}) = 0.1946$.

d) The width of η_b can now be bounded as

$$\Gamma(\,\eta_b \to 2g\,) = \frac{32\pi}{3}\,\frac{\alpha_s^2}{M^2_{Q\bar{Q}}}\,|\phi_s^b(0)|^2$$

$$< \;40 \text{ MeV} \quad . \tag{4.22}$$

e) It may be noted that the potential of Gupta for the S-states quarkonia can also be written in the form

$$V \;=\; V_o(r) + V_\sigma(\,S^2 - \tfrac{3}{4}\,) \tag{4.23}$$

with $\dfrac{dV_o}{dr} > 0$, $\dfrac{d^2V_o}{dr^2} < 0$, $\dfrac{dV_\sigma}{dr} < 0$. Thus the first inequality $\phi_s^b(0) > \phi_t^b(0)$, should also hold.

f) The value of $\phi_t^b(0)$ is already known (from its leptonic decay width), $|\phi_t^b(0)|^2 \approx 0.403$ GeV^3. We, therefore, get a lower bound for

$$\Gamma(\,\eta_b \to 2g\,) \;>\; 5.7 \text{ MeV} \quad , \tag{4.24}$$

g) Rosner *et al.*[100] obtained the inequality

$$\psi^2_{M'}(0) \geq \frac{M'}{M}\psi^2_M(0) \qquad (4.25)$$

which is valid for power-law potentials and also for the class of potentials discussed in this chapter. We have given elsewhere[97] a proof of this inequality for more general potentials. Since $\psi^2(0)$ for $^1S_0$ $c\bar{c}$ state is $\sim$ 0.0651 GeV^3, we obtain the bound

$$\Gamma(\eta_b \to 2g) > 3.23 \text{ MeV} \qquad (4.26)$$

which is, however, weaker than the bound in (4.24).

IV.4. Conclusions :

We have presented in this chapter some general results on the hyperfine members of the S-states quarkonia for a general class of potentials. The results will be valid even if the Breit-Fermi form of the spin-dependent potential is not valid. We first use a flavour-independent potential and obtain a lower bound on the wave-function of the singlet S-states of $b\bar{b}$. We consider in this context Gupta's potential for the $Q\bar{Q}$ system and make use of the mass-scaling properties of the relevant Schrödinger equation to predict that the width $\Gamma(\eta_b \to 2g)$ should lie within the range 6 $\sim$ 40 MeV. Thus even the weak inequalities considered here are useful in quarkonium spectroscopy.

* CHAPTER V

TWO GLUINO BOUND STATES

* A part of the contents of this chapter has already been published in Ref.(97).

V.1. Introduction :

Supersymmetric QCD gives a simple method of studying the two gluino ($\tilde{g}\tilde{g}$) bound states. The production and decay rates of $\tilde{g}\tilde{g}$ states have already been studied by a number of authors.[58] The gluinos are expected to have a long life and can, therefore, form bound states which may be detected. The study of $\tilde{g}\tilde{g}$ states is expected to provide a simple method of detecting a sparticle. However, there are considerable uncertainties in the theoretical predictions for the $\tilde{g}\tilde{g}$ states, which stem from the uncertainties in the gluino mass $\mu_{\tilde{g}}$ as well as in the two gluino potential, $V_{\tilde{g}\tilde{g}}$. The speculations about the gluino mass have been centred around 5 GeV (light gluino) or 60 GeV (heavy gluino), with the experimental bias shifting towards a heavier gluino.[101] For these gluino masses, non-relativistic bound state model is adequate to predict wave-functions and binding energies of $\tilde{g}\tilde{g}$ states. The potential for the $\tilde{g}\tilde{g}$ system is only partially known. A simple minded application of supersymmetric QCD to the gluino sector suggests that the short-distance part of the $\tilde{g}\tilde{g}$ potential is related to the short-distance part of the quark-antiquark potential by the colour factor 9/4. There is, however, no such relation for the long-range part of the potentials. Some authors[58,59] have assumed the same proportionality constant 9/4 between the two potentials, even for the non-perturbative long-range part, just because it makes the total $V_{\tilde{g}\tilde{g}}$ potential

proportional to the $Q\bar{Q}$ potential, $V_{Q\bar{Q}}$. Since there is a quark in each of the mass ranges presently considered for the gluino, it is indeed convenient to study the $\tilde{g}\tilde{g}$ states by comparing with the quarkonium states, which are rather well-studied. In the hadron colliders, $\tilde{g}\tilde{g}$ states may be produced via the $gg \to \tilde{g}\tilde{g}$ and $Q\bar{Q} \to \tilde{g}\tilde{g}$ subprocesses. Goldman and Haber[102] discussed the method of detection of the gluinonium states which may be produced in hadron collider and in quarkonium decay. A convenient method of detecting the $\tilde{g}\tilde{g}$ states will be to look for a radiative decay, $(t\bar{t}) \to \gamma + \tilde{g}\tilde{g}(^1S_0)$, if permitted kinematically. To estimate this and other decay widths and production crossection, one needs the particle density at the origin, $|\psi_{\tilde{g}\tilde{g}}(0)|^2$ of the $\tilde{g}\tilde{g}$ states. The uncertainty in the contribution of the long-range potential makes any theoretical prediction for $|\psi_{\tilde{g}\tilde{g}}(0)|^2$ unreliable. We shall show by considering a particular potential model that there is a significant dependence of the theoretical results on the long-range potential. Given this situation, it seems reasonable to look for model independent results or bounds. The observation that heavy quarkonia can be described by a Schrödinger equation with a non-relativistic $Q\bar{Q}$ potential has led to considerable activities in the study of general properties of the Schrödinger equation with confining potentials. The scaling properties of the Schrödinger equation for power-law potentials have been found[6] to be very useful in deriving results of this nature. Rigorous results on level ordering for more general potentials have been obtained by Grosse and Martin.[98] The value of the S-states

wave-function at the origin $\psi(0)$ has a special significance in quarkonium spectroscopy as this quantity occurs in the expressions for various decay widths of the state. Martin has obtained rigorous results for the relative magnitudes of the wave-function at the origin for 1S and 2S states for the usual quarkonium potentials. Martin[103] has, in particular, shown that for convex (concave) $Q\bar{Q}$ potentials, $|\psi_{2S}(0)| > |\psi_{1S}(0)|$ $\left(|\psi_{2S}(0)| < |\psi_{1S}(0)|\right)$ which was found useful in comparing the leptonic decay widths of the quarkonia. Some of the techniques used by Martin are now familiar and we shall use them to derive some inequalities relevant for the study of $\tilde{g}\tilde{g}$ states. The purpose of this chapter is to point out that the results can be generalised further to obtain some useful information about the two gluino bound states.

The presentation in the remaining part of this chapter is as follows. In section V.2, the two gluino bound state potential is briefly reviewed. In section V.3, we consider a class of potentials to study the effect of the long-range part of the potential on the spectroscopy of the two gluino system, using some general properties of the Schrödinger equation. The results may provide bounds on decay widths. The last section gives our conclusions.

V.2. Two gluino bound state :

Gluinos are a self-conjugate majorana spinor, transforming

as an octet of colour SU(3) and are supersymmetric partners of gluons. It would be exactly massless at the tree level if supersymmetry were an unbroken symmetry. The gluino-gluino bound states are known to follow the general decomposition rule

$$8 \times 8 = 1 + 8_S + 8_A + 10 + 10^* + 27 \ .$$

We, however, need consider only the singlet sector. Starting from an octet QCD action, Zuk *et al.*[58] followed the method of Brink *et al.*[104] to extend the original QCD lagrangian to the supersymmetric sector. The action is given by

$$S = \int d^4x \ [- \frac{1}{4} F^a_{\mu\nu} F^{\mu\nu}_a + \frac{i}{2} \bar{\tilde{g}}^a \gamma.D \tilde{g}_a]$$

which describes the interaction between the SU(3) gauge vector boson and its superpartner gluino fields. D_μ is a covariant derivative, $D_\mu = \partial_\mu + ig \ T^a.A^a_\mu$ and $F^a_{\mu\nu}$ (a = 1,2,------8) are the Yang-Mills fields constructed from the adjoint representation of gluon field. T^a are colour matrices. The gluino (majorana) field $\tilde{g}_a$ satisfies the condition $\tilde{g}^a = c\bar{\tilde{g}}^{aT}$ which is necessary to halve the number of fermionic degrees of freedom to match the number of bosonic degrees of freedom. The majorana constraint is SU(3) gauge invariant. The interaction lagrangian term of gluino and gluon is obtained as

$$L_{int} = -g \ J^\mu_a \ A^a_\mu$$

where J^{μ}_{a} is a gluino current, written as $J^{\mu}_{a}(x) = \frac{1}{2} \bar{\tilde{g}}(x)\gamma^{\mu}T_{a}\tilde{g}(x)$ and g is the strong QCD coupling constant. The matrix elements of the gluino current is

$$\langle \tilde{g}' | : J^{a}_{\mu}(0) : | \tilde{g} \rangle = T^{a}\bar{u}(k's')\gamma_{\mu}u(ks)$$

where k and s denote the momentum and spin of the free gluino states. We now consider $\tilde{g}\tilde{g}$ scattering at the one-gluon-exchange level. The relevant diagram gives the matrix element

$$M_{fi} = g^{2}\left[\frac{1}{8}\,\mathrm{Tr}\sum_{a}(T^{a})^{2}\right]\frac{1}{q^{2}}\,\bar{u}(k_{2}'s_{2}')\gamma^{\mu}u(k_{2}s_{2})\bar{u}(k_{1}'s_{1}')\gamma_{\mu}u(k_{1}s_{1}) .$$

Comparing this matrix element with that for $e^{-}e^{-}$ scattering with one-photon-exchange, we see that

$$V_{\tilde{g}\tilde{g}} = -C_{2}(G)g^{2}\,V_{e^{-}e^{-}}\,|_{e^{2}=1} .$$

Considering a similar graph for $Q\bar{Q} \to Q\bar{Q}$, we note the scaling relation

$$V_{\tilde{g}\tilde{g}} = C_{2}(G)/C_{2}(R)\;V_{Q\bar{Q}} = 9/4\;V_{Q\bar{Q}} . \qquad (5.1)$$

The above relation is valid for large Q^{2}, in the region of perturbative QCD. But at small Q^{2}, we have no knowledge of QCD potential and the scaling relation need not hold for the long distance part of the potential. In the next section, we show the dependence of the theoretical results on the undetermined long-

range part of the potential.

V.3. Long-range potential and results :

To study the effect of the long-range part of the potential, we consider a simple parametrization by assuming that

$$V_{Q\bar{Q}} = V_S(r) + V_L(r) \quad , \tag{5.2}$$

$$V_{gg} = \alpha\, V_S(r) + \beta\, V_L(r) \quad , \tag{5.3}$$

where α, β are real parameters. $V_S(r)$ is the short-range potential, which is attractive and dominant near $r = 0$. The long-range part, $V_L(r)$ becomes positive and divergent as $r \to \infty$. We first consider a particular non-relativistic potential $V_{Q\bar{Q}} = V_S + V_L$, with

$$V_S(r) = f(r)\, V_{QCD}^{(2)}(r) \quad , \qquad V_L(r) = \left(1 - f(r)\right) V_M(r) \tag{5.4}$$

$$\text{and} \qquad f(r) = \frac{\left(1 + e^{-a/s}\right)}{\left(1 + e^{(r-a)/s}\right)}$$

where V_S is estimated from the two-loop QCD calculations, given by the Eq. (2.3). We choose $\Lambda_{\overline{MS}} = 0.200$ GeV and $N_f = 4$. In (5.4), V_M is a Martin-type power-law potential given by

$$V_M(r) = -7.392 + 8.080 r^{0.1} \tag{5.5}$$

with r in fm. The choice is motivated so that

$$V_{QCD}(r=a) = V_M(r=a) \ . \qquad (5.6)$$

We have chosen the parameters in the potentials V_S and V_L so that the condition (5.6) is satisfied. Because of this condition, the calculated spin-averaged results are not very sensitive to the choice of the values of a and s.[66] We have chosen a = 0.0723 fm and s = 0.01 fm in the following calculations. The singularity of $V^{(2)}_{QCD}(r)$ at $r = \Lambda^{-1}_{\overline{MS}}$ should be ignored in calculating $V_S(r)$. One may truncate $V_S(r)$ for $r > r_o$, where one chooses $r_o < \Lambda^{-1}_{\overline{MS}}$ so that $(r_o - a)/s \gg 1$. The results are then insensitive to the value of r_o chosen.

We now assume $V_{\tilde{g}\tilde{g}} = 9/4\ V_S + \beta\ V_L$ and calculate the binding energies and the values of $|\psi_{\tilde{g}\tilde{g}}(0)|^2$ of the $\tilde{g}\tilde{g}$ system for a range of β values ($0.5 \leq \beta \leq 3$)and with different gluino mass. Our results are shown in Figs.5.1-5.4. We do not expect a large deviation for these results for any other acceptable potential model. We note, in particular, that $|\psi(0)|^2$ for both light and heavy gluinos show a significant dependence on β. It is obvious that the long-range part needs more attention.

The decay rates of gluinonium are given by expressions similar to those of the corresponding quarkonia, apart from the group factors

$$\frac{1}{2}\ \frac{8}{3}\ |\ c_2(G)\ /\ c_2(R)\ |^2 = 27/4 \ .$$

Thus the decay width of two gluino bound state is given by

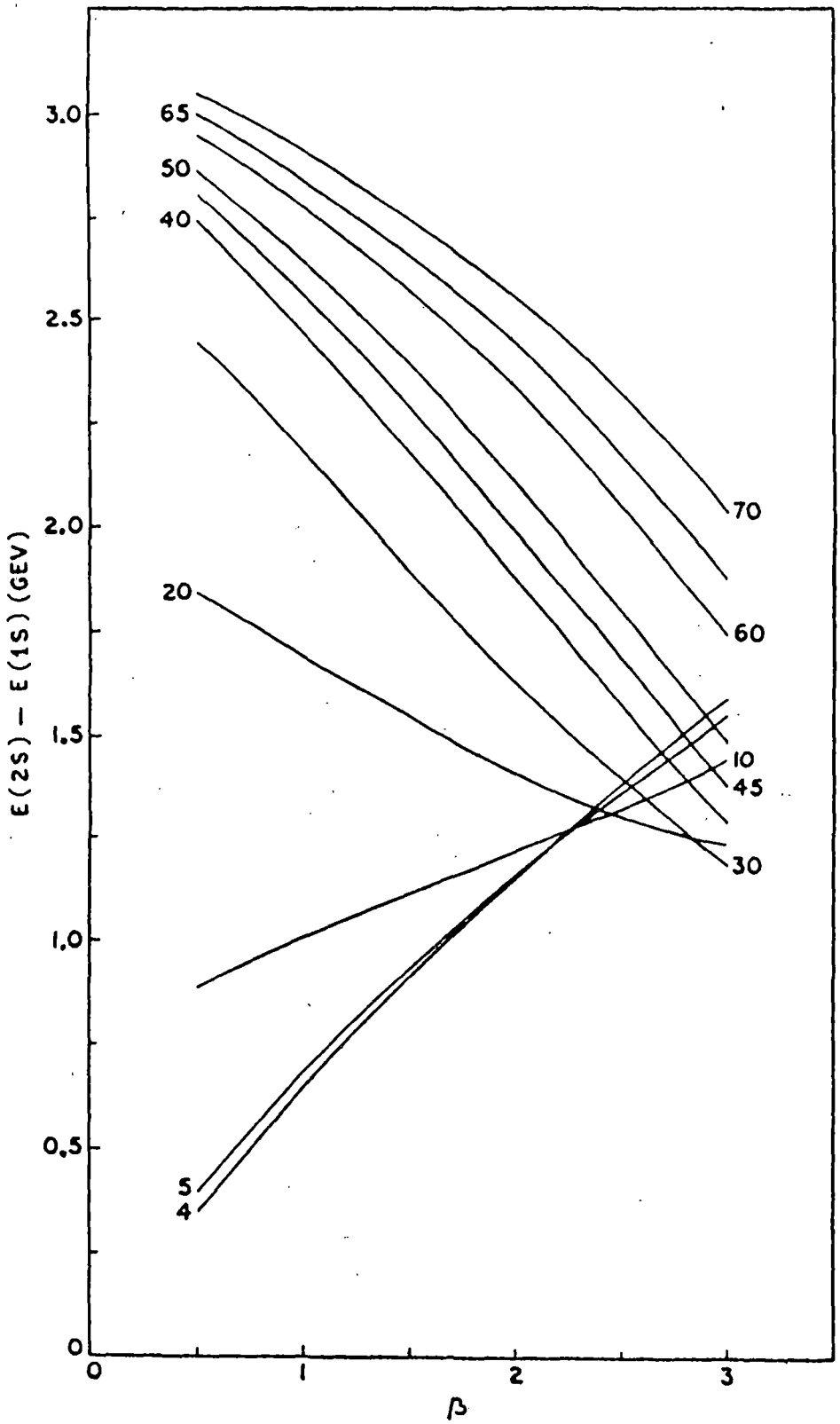

Fig.5.1. The energy level separation, E(2S) − E(1S), of the $\tilde{g}\tilde{g}$ system for $0.5 \leq \beta \leq 3$. The numbers indicate the gluino mass $\mu_{\tilde{g}}$ in GeV.

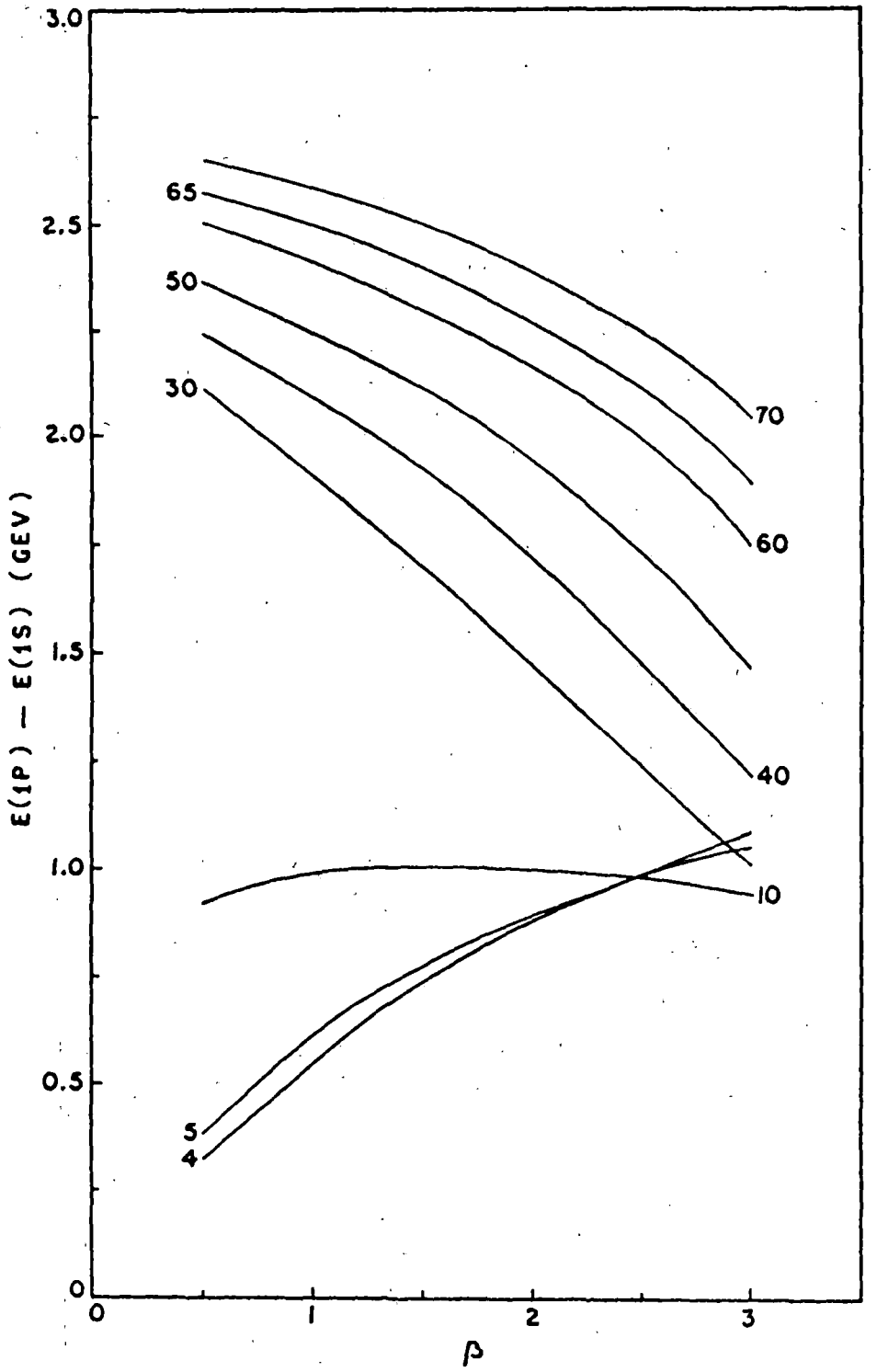

Fig.5.2. The level separation $E(1P) - E(1S)$ of the $\tilde{g}\tilde{g}$ system for $0.5 \leq \beta \leq 3$. The numbers indicate $\mu_{\tilde{g}}$ in GeV.

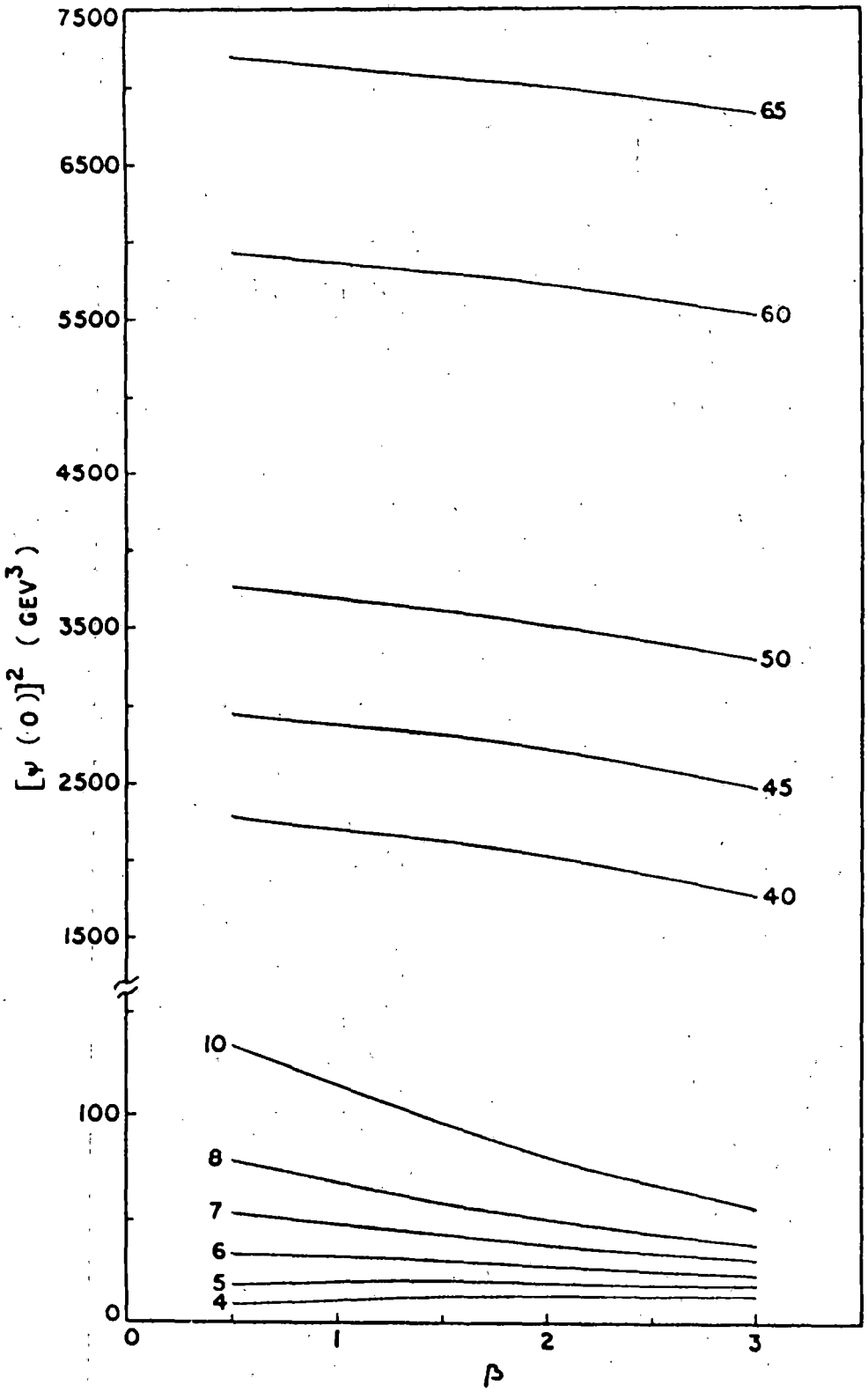

Fig.5.3. The values of $|\psi(0)|^2$ for the $\tilde{g}\tilde{g}$ 1S state. The numbers indicate $\mu_{\tilde{g}}$ in GeV.

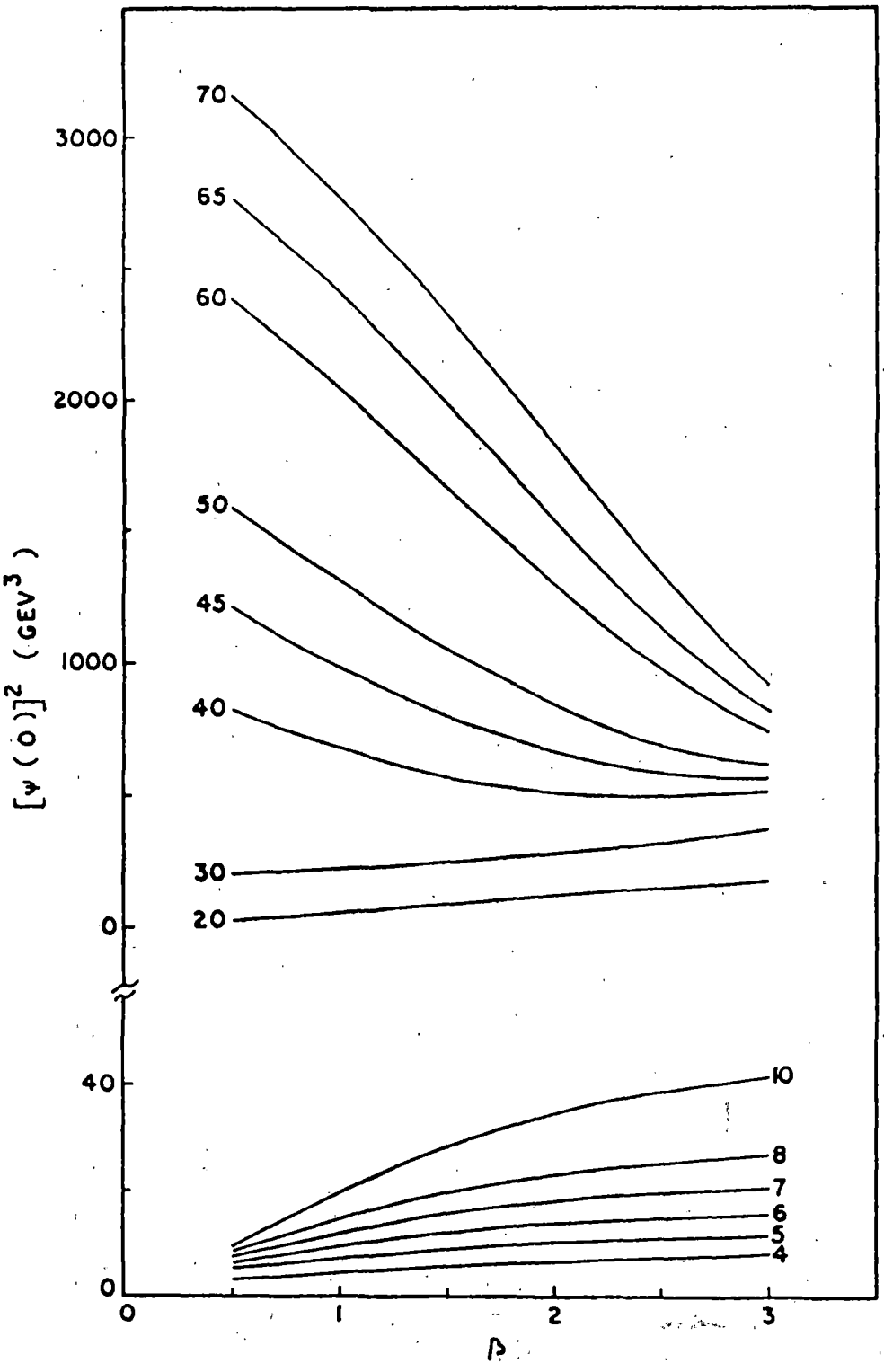

Fig.5.4. The values of $|\psi(0)|^2$ for the $\tilde{g}\tilde{g}$ 2S state. The numbers indicate $\mu_{\tilde{g}}$ in GeV.

$$\Gamma(\tilde{g}\tilde{g}(0^{-+}) \rightarrow gg) = \frac{27}{4}\frac{8}{3}\alpha_s^2 |\psi_{\tilde{g}\tilde{g}}(0)|^2/M^2 . \qquad (5.7)$$

The standard formula for $\tilde{g}\tilde{g}$ production cross-section in hadron collisions is

$$\sigma = (2J+1)\pi^2\frac{\Gamma(\tilde{g}\tilde{g} \rightarrow gg)}{8M^3}\int_\tau^1 \frac{dx}{x}\tau\, f_g(x)\, f_g(\tau/x) \qquad (5.8)$$

where $\tau = M^2/S$, M, the gluinonium mass and $3(1-x)^5/x$ is assumed to give the distribution function for gluons. We have considered only the cross-section for pseudoscalar production. We have shown in Fig.5.5, the cross-section versus $\mu_{\tilde{g}}$ for two different beam energies ($\sqrt{S}$) considering two different values of β. An increase in β decreases the cross-section for a given gluino mass. Our calculated results agree with those of Kühn and Ono[58] but differ slightly from the results of Kane and Leveille[105] at a higher beam energy.

A study of the general features of the potentials (5.2) and (5.3) provides some information which may be obtained in the form of inequalities. The proof of the inequality makes use of the techniques developed by Martin. We assume that both the short-range and the long-range parts of the potential are monotonically increasing. The assumption is true for almost all the potential models considered for the $Q\bar{Q}$ systems. Thus V_S and V_L in (5.2) and (5.3) satisfy

$$\frac{dV_S}{dr} > 0 \quad , \quad \frac{dV_L}{dr} > 0 \qquad (5.9)$$

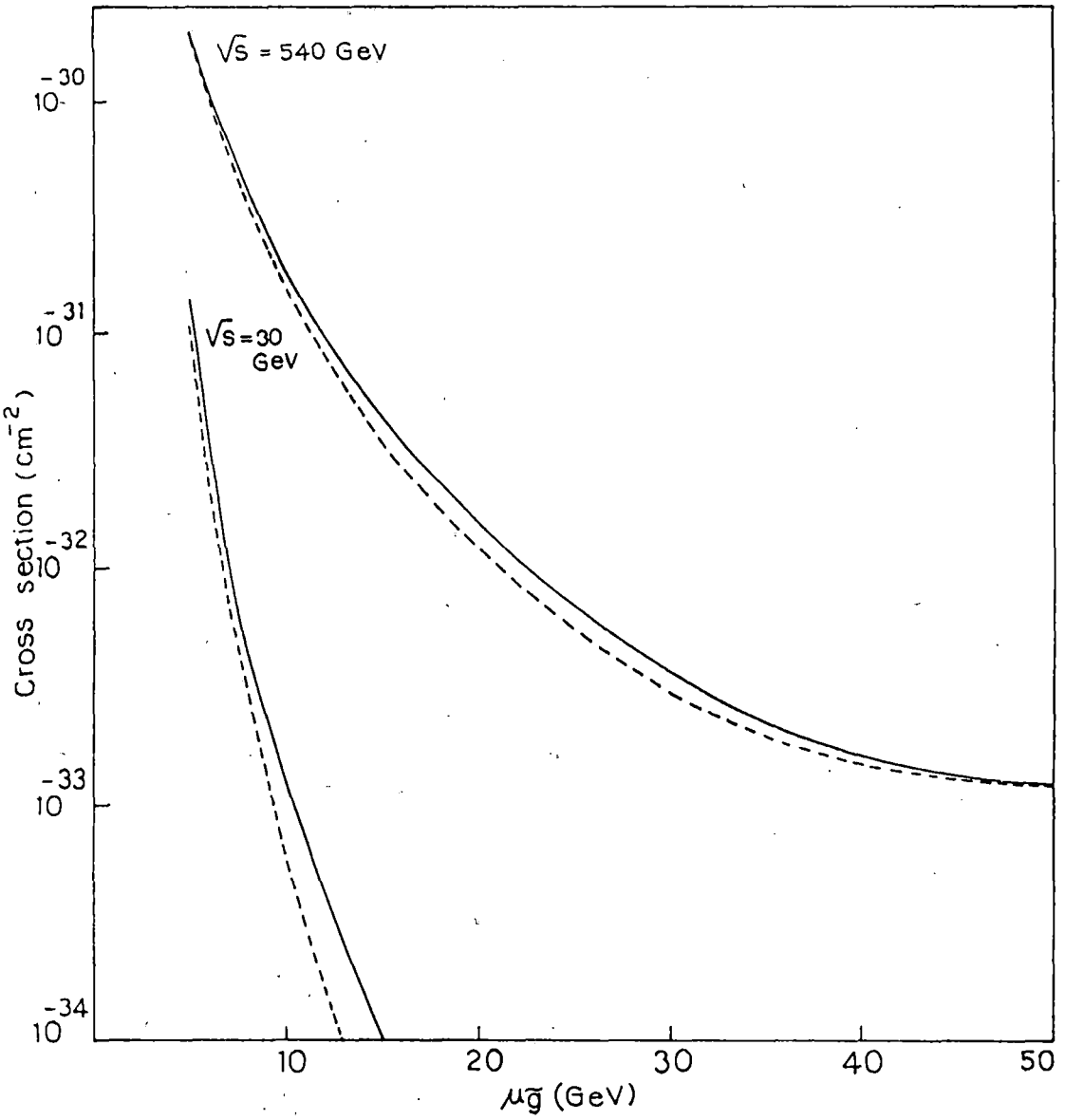

Fig.5.5. The values of cross-section(σ) for pseudoscalar production VS. $\mu_{\tilde{g}}$. The solid line corresponds to β=2.25 and the broken line to β=3 .

and $\dfrac{d^2 V_{\tilde{g}\tilde{g}}}{dr^2} < 0$ (concave downwards) (5.10)

but are otherwise arbitrary. We can derive the following results:

(a) If $\mu_{\tilde{g}}/\mu_Q > 1/\alpha$ and $\beta > \mu_Q/\mu_{\tilde{g}}$,

we have for the 1S states

$$|\psi_{\tilde{g}\tilde{g}}(0)|^2 > \text{Min}(\alpha,\beta)(\mu_{\tilde{g}}/\mu_Q)\,|\psi_{Q\bar{Q}}(0)|^2 , \quad (5.11)$$

where Min(α,β) is the smaller of the two parameters.

(b) If $\mu_{\tilde{g}}/\mu_Q < 1/\alpha$ and $\beta < \mu_Q/\mu_{\tilde{g}}$,

$$|\psi_{\tilde{g}\tilde{g}}(0)|^2 < |\psi_{Q\bar{Q}}(0)|^2 . \quad (5.12)$$

Let $\psi_{\tilde{g}\tilde{g}} = v(r)/r$ and $\psi_{Q\bar{Q}}(r) = u(r)/r$ be the 1S radial solutions for the $\tilde{g}\tilde{g}$ and $Q\bar{Q}$ systems respectively. Both u abd v are chosen positive. To prove the inequality (5.11), we follow the steps outlined below:

(i) For $r \to \infty$, we can make use of the large r behavior of the radial equations to show that $v^2 < u^2$ for $r \to \infty$, if $\beta > \mu_Q/\mu_{\tilde{g}}$.

(ii) It can be shown that $v^2 - u^2$ has a unique zero. Consider the Wronskian

$$I(r) = (v'u - u'v)(r)$$

$$= \frac{1}{\hbar^2}\int_0^r uv\,\Big[\,(\alpha\,\mu_{\tilde{g}} - \mu_Q)V_S + (\beta\,\mu_{\tilde{g}} - \mu_Q)V_L$$

$$- (E'\,\mu_{\tilde{g}} - E\,\mu_Q)\,\Big]\,dr . \quad (5.13)$$

Since $I(\infty) = 0$, we may also write the following representation

$$I(r) = -\frac{1}{\hbar^2}\int_r^\infty uv\left[(\alpha\,\mu_g^{\sim} - \mu_0)V_S + (\beta\,\mu_g^{\sim} - \mu_0)V_L\right.$$

$$\left. - (E'\,\mu_g^{\sim} - E\,\mu_0)\right]dr \quad . \qquad (5.14)$$

From (5.13), it follows that for $r \sim 0$, the integrand is $\sim (\alpha\,\mu_g^{\sim} - \mu_0)V_S$ and negative and hence $I(r) < 0$. For $r \to \infty$, one finds that the integrand is $\sim (\beta\,\mu_g^{\sim} - \mu_0)V_L$ and hence from (5.14), it follows that $I(r)$ is also negative at large r. Since both V_S and V_L are monotonic, u and v are nonzero and positive. It has, therefore, only one zero, say at $r = r_0$. For $r < r_0$, we use the relation (5.13) and for $r > r_0$, we use the relation (5.14) to show that $I(r) < 0$ for all r. We can now show that $v - u$ vanishes only once, say at $r = r_1$. The relation (5.13) gives

$$u(r_1)\left[v'(r_1) - u'(r_1)\right] < 0 \quad . \qquad (5.15)$$

Thus $(v' - u')_{r=r_1} < 0$, since $u > 0$. The uniqueness of the zero of $v - u$ and hence of $(v^2 - u^2)$ follows from above.

(iii) Since $v^2 - u^2 < 0$ for $r \to \infty$ and since $v^2 - u^2$ has a unique zero, we conclude that $v^2 - u^2 > 0$, for $r \sim 0$.

(iv) In the last step, we make use of the well-known relations like

$$u'^2(0) = \frac{\mu_0}{\hbar^2}\int u^2\,\frac{dV}{dr}\,dr \quad . \qquad (5.16)$$

We consider, with $\beta \leq \alpha$,

$$|\psi^{\sim\sim}_{gg}(0)|^2 - \beta \frac{\mu^{\sim}_g}{\mu_Q} |\psi_{Q\bar{Q}}(0)|^2$$

$$= v'^2(0) - \beta \frac{\mu^{\sim}_g}{\mu_Q} u'^2(0)$$

$$= \frac{\mu^{\sim}_g}{\hbar^2} \int dr \ (v^2 - u^2) \frac{dV^{\sim\sim}_{gg}}{dr} + \frac{\mu^{\sim}_g}{\hbar^2} \int dr \ u^2(\alpha - \beta) \frac{dV_S}{dr}$$

$$\geq \frac{\mu^{\sim}_g}{\hbar^2} \int dr \ (v^2 - u^2) \left[\frac{dV^{\sim\sim}_{gg}}{dr} - \frac{dV^{\sim\sim}_{gg}}{dr}\Big|_{r=r_1} \right]$$

$$> 0 \ ,$$

since

$$\frac{d^2 V^{\sim\sim}_{gg}}{dr^2} < 0 \ . \qquad (5.17)$$

For $\beta > \alpha$, we can show that

$$|\psi^{\sim\sim}_{gg}(0)|^2 - \alpha \ (\mu^{\sim}_g/\mu_Q) \ |\psi_{Q\bar{Q}}(0)|^2$$

is positive definite. This completes the proof of the inequality (5.11). For $\mu^{\sim}_g/\mu_Q < 1/\alpha$, $\beta < \mu_Q/\mu^{\sim}_g$, we may follow the same steps to derive an upper bound for $|\psi^{\sim\sim}_{gg}(0)|^2$, *viz.* the inequality (5.12). Our results are shown explicitly in Fig.5.6 for $\alpha = 9/4$. We cannot make any prediction for the striped regions. We note the following:

(i) For quarkonium states, an useful inequality for two $Q\bar{Q}$ states

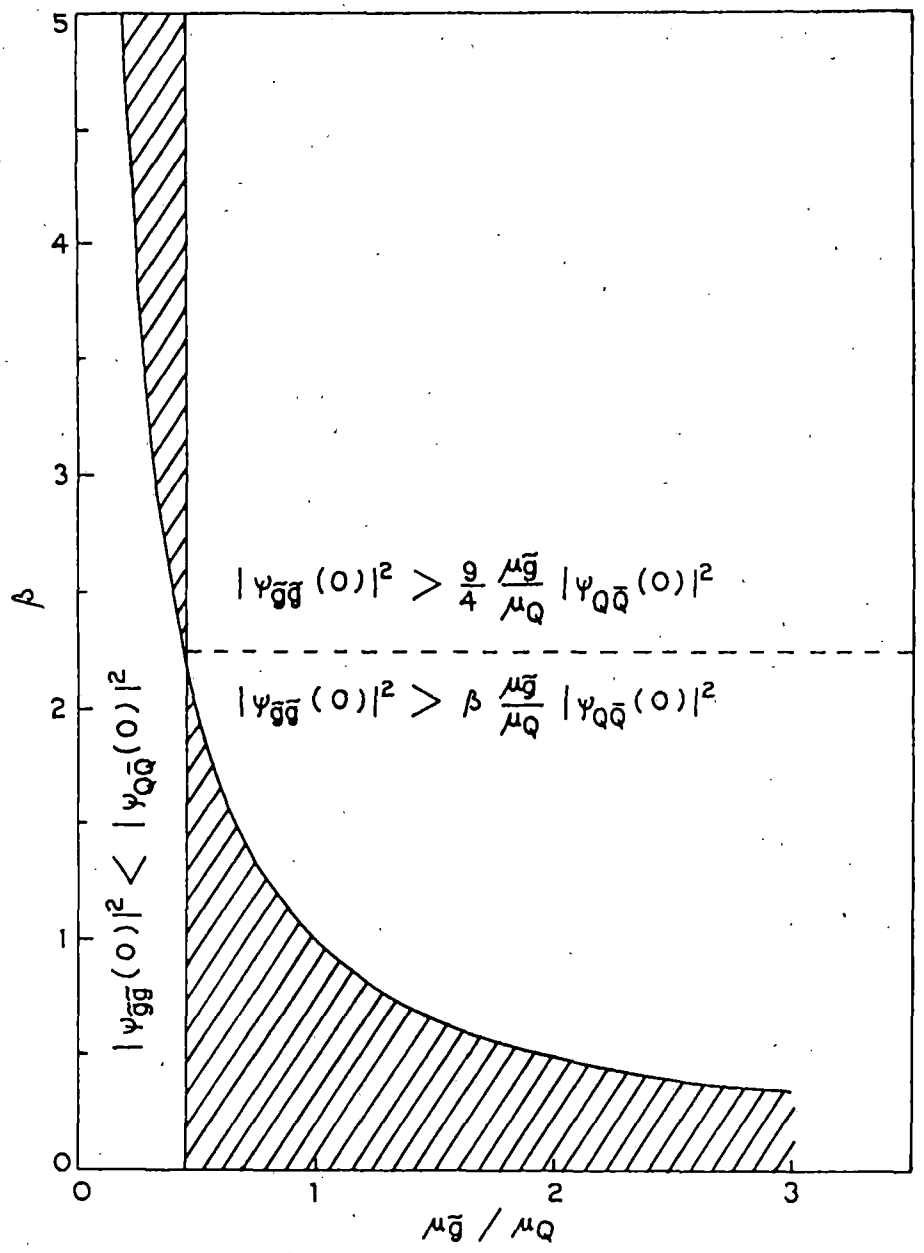

Fig.5.6. The inequalities (5.11) and (5.12) shown explicitly. There is no prediction for the striped region.

with masses μ_Q and $\mu_{Q'}$ was considered by Rosner *et al.*[100]

$$\psi^2_{Q',\bar{Q}'}(0) \geq \frac{\mu_{Q'}}{\mu_Q} \psi^2_{Q\bar{Q}}(0) , \qquad \mu_{Q'} > \mu_Q . \tag{5.18}$$

The inequality has been shown to be valid for power-law potentials and also for a potential satisfying conditions like (5.9) and (5.10) in the WKB approximation. Our results, with $\alpha = \beta = 1$ provide a rigorous proof of this inequality for a large class of potentials.

(ii) For $\mu_{\tilde{g}} \simeq \frac{4}{9} \mu_t$ we have the equality $\psi_{\tilde{g}\tilde{g}}(0) = \psi_{t\bar{t}}(0)$ for $\beta = 9/4$. For a smaller β, $\psi_{t\bar{t}}(0) > \psi_{\tilde{g}\tilde{g}}(0)$, while for a larger β, the situation is reversed. The variation of $\psi(0)$ with β is expected to be smooth, as has also been seen in our model calculations.

(iii) The results may be useful for estimating bounds on decay widths. As an example, consider the two gluon decay width (5.7). Suppose $\beta \sim 9/4$ and $\mu_t = 45$ GeV. If $\mu_{\tilde{g}} = 20$ GeV,

$$\Gamma(\tilde{g}\tilde{g}(0^{-+}) \to gg) \simeq 190 \text{ MeV}, \tag{5.19}$$

where we have used the result $|\psi_{t\bar{t}}(0)|^2_{1S} = 350$ GeV^3, as can be seen from calculations with the potential (5.4). This may be compared with the two gluon width of the 1S toponium state for $\mu_t \sim 45$ GeV which is about 5 MeV. The latter estimate is in general agreement with the results of Nanopoulos *et al.*,[59] who consider a particular $Q\bar{Q}$ potential. Combining the inequalities of Fig.5.6 with the results (5.19), we can now derive some crude bounds on

the decay widths. The knowledge of $\mu_{\tilde{g}}$ (or some strict constraints on $\mu_{\tilde{g}}$) will help in making the predictions sharper. If $\mu_{\tilde{g}}/\mu_t \gtrsim 1$, the inequalities become valid for larger ranges of β.

(iv) For the class of potentials considered, Martin has proved that $\psi_{2S}(0) > \psi_{1S}(0)$. Thus we can obtain a weak inequality if we replace $\psi_{\tilde{g}\tilde{g}}(0)$ of 1S state by $\psi_{\tilde{g}\tilde{g}}(0)$ for 2S state in the relation (5.11).

V.4. Conclusions:

We have shown that the long-range part of the $\tilde{g}\tilde{g}$ potential may affect significantly the theoretical prediction for $|\psi_{\tilde{g}\tilde{g}}(0)|^2$. We have also studied the dependence of the binding energy difference and the value of the wave-function at the origin on the gluino mass for various values of β ($0.5 \leq \beta \leq 3$). Although, the long-range part of the $\tilde{g}\tilde{g}$ potential is not known, it is interesting to note that by using Martin's technique, one can derive useful inequalities relevant for the study of $\tilde{g}\tilde{g}$ states. The inequality holds for a range of values of β and $\mu_{\tilde{g}}/\mu_Q$ as shown in Fig.5.6. In fact, in the absence of any definite information about either $\mu_{\tilde{g}}$ or β, the theoretical predictions will perhaps be no better than the predictions of the inequalities shown in Fig.5.6.

CHAPTER VI

REFERENCES

1. H. D. Politzer , Phys. Rev. Lett. 30 (1973) 1346 ; D. J. Gross and F. Wilczek , Phys. Rev. Lett. 30 (1973) 1343 .
2. A. J. Buras , Rev. Mod. Phys. 52 (1980) 199 .
3. T. Goto, Prog. Theor. Phys. 46 (1971) 1560 ; A. Neveu and J. H. Schwarz , Nucl. Phys. B 31 (1971) 86 ; P. Ramond, Phys. Rev. D 3 (1971) 2415 .
4. S. L. Adler and T. Piran , Rev. Mod. Phys. 56 (1984) 1 ; M. Baker , J. S. Ball and F. Zachariasen , Phys. Rev. D 31 (1985) 2575 ; D 34 (1986) 3894 .
5. M. Creutz , Phys. Rev. Lett. 45 (1980) 313 ; G. Münster and P. Weisz , Phys. Lett. 96B (1980) 119 ; J. Kogut and L. Susskind , Phys. Rev. D 11 (1975) 395 .
6. C. Quigg and J. L. Rosner , Phys. Rep. C 56 (1979) 167 and references therein .
7. A. Martin, Phys. Lett. 93B (1980) 338 ; 100B (1981) 511 .
8. A. Khare , Phys. Lett. 98B (1981) 385 .
9. S. L. Glashow , Nucl. Phys. 22 (1961) 579 ; S. Weinberg , Phys. Rev. Lett. 19 (1967) 1264 .
10. T. Appelquist and H. D. Politzer , Phys. Rev. Lett. 34 (1975) 43 .
11. S.E. Baru *et al.*, Z. Phys. C 30 (1986) 551 ; A. S. Artamonov, Phys. Lett. 137B (1984) 272 .
12. S. E. Baru *et al.*, Z. Phys. C 32 (1986) 662 .
13. D. P. Barber *et al.*, Phys. Lett. 135B (1984) 498 .
14. C. Bebek *et al.*, Phys. Rev. D 36 (1987) 1289 .
15. C. Klopfenstein *et al.*, Phys. Rev. Lett. 51 (1983) 160 ; F.

Pauss *et al.*, Phys. Lett. 130B (1983) 439 .

16. P. Hass *et al.*, Phys. Rev. Lett. 52 (1984) 799 .

17. H. Albrecht *et al.*, Phys. Lett. 160B (1985) 331 .

18. R. Nernst *et al.*, Phys. Rev. Lett. 54 (1985) 2195 .

19. W. Walk *et al.*, Phys. Rev. D 34 (1986) 2611 .

20. J. Lee-Franzini , CUSB Collaboration , Hamburg Conf. (1987) .

21. CLEO Collaboration : T. Bowcock *et al.*, Phys. Rev. Lett. 58 (1987) 307 .

22. C. Baglin *et al.*, Nucl. Phys. B 286 (1987) 592 ; A. A. Zholentz *et al.*, Phys. Lett. 96B (1980) 214 .

23. C. Baglin *et al.*, Phys. Lett. 187B (1987) 191 ; 172B (1986) 455 .

24. J. E. Gaiser *et al.*, Phys. Rev. D 34 (1986) 711 .

25. C. Edwards *et al.*, Phys. Rev. Lett. 48 (1982) 70 .

26. R. H. Schindler *et al.*, Phys. Rev. D 21 (1980) 2716 ; W. Bacino *et al.*, Phys. Rev. Lett. 40 (1978) 671 .

27. C. Baglin *et al.*, Phys. Lett. 171B (1986) 135 .

28. Particle Data Group , Review of Particle Properties , Phys. Lett. 170B (1986) 1 ; 204B (1988) 1 .

29. G. Arnison *et al.*, Phys. Lett. 147B (1984) 493 .

30. R. Van Royen and V. F. Weisskopf , Nuovo Cimento 50 (1967) 617 ; 51 (1967) 583 .

31. E. Eichten , K. Gottfried , T. Kinoshita , K. D. Lane , T.-M. Yan , Phys. Rev. Lett. 36 (1976) 500 ; E. Eichten and K. Gottfried , Phys. Lett. 66B (1977) 286 ; E. C. Poggio and H. J. Schnitzer , Phys. Rev. Lett. 41 (1978) 1344 ; Phys. Rev.

D 19 (1979) 1557 ; D 20 (1979) 1175 ; A. Billoire and A. Morel , Nucl. Phys. B 135 (1978) 131 ; W. Celmaster , H. Georgi and M. Machacek , Phys. Rev. D 17 (1978) 879 .

32. E. Eichten , K. Gottfried , T. Kinoshita , K. D. Lane and T. -M. Yan, Phys. Rev. D 17 (1978) 3090 ; D 21 (1980) 203 .

33. E. E. Salpeter and H. A. Bethe , Phys. Rev. 84 (1951) 1232 .

34. J. Pumplin , W. Repko and A. Sato, Phys. Rev. Lett. 35 (1975) 1538 ; H. J. Schnitzer , Phys. Rev. Lett. 35 (1975) 1540 ; Phys. Rev. D 13 (1976) 74 .

35. D. Gromes , Nucl. Phys. B 131 (1977) 80 ; J. Sucher , Rep. Prog. Phys. 41 (1978) 1781 .

36. A. B. Henriques , B. H. Kellett and R. G. Moorhouse , Phys. Lett. 64B (1976) 85.

37. H. Ito , Prog. Theor. Phys. 70 (1983) 499 ; 75 (1986) 1416 ; 76 (1986) 567 ; A. N. Mitra , Z. Phys. C 8 (1981) 25 ; S. Ishida , H. Kakuhata and S. Naka , Prog. Theor. Phys. 75 (1986) 1204 .

38. E. E. Salpeter , Phys. Rev. 87 (1952) 328 .

39. A. Mittal and A. N. Mitra , Phys. Rev. Lett. 57 (1986) 290 .

40. S. Jacobs , M. G. Olsson and C. J. Suchyta III , Phys. Rev. D 35 (1987) 2448 .

41. E. Eichten and F. L. Feinberg , Phys. Rev. Lett. 43 (1979) 1205 ; Phys. Rev. D 23 (1981) 2724 .

42. D. Gromes , Z. Phys. C 26 (1984) 401 .

43. D. Gromes , Z. Phys. C 22 (1984) 265 .

44. W. Buchmüller , Phys. Lett. 112B (1982) 479 .

45. P. Moxhay and J. L. Rosner , Phys. Rev. D 28 (1983) 1132 .

46. R. McClary and N. Byers , Phys. Rev. D 28 (1983) 1692 .

47. J. Pantaleone , S.-H.H. Tye and Y. J. Ng , Phys. Rev. D 33 (1986) 777 .

48. S. N. Gupta and S. F. Radford , Phys. Rev. D 24 (1981) 2309 ; D 25 (1982) 3430 .

49. S. N. Gupta , S. F. Radford and W. W. Repko , Phys. Rev. D 26 (1982) 3305 .

50. K. Igi and S. Ono , Phys. Rev. D 33 (1986) 3349 .

51. L. P. Fulcher , Phys. Rev. D 37 (1988) 1258 .

52. A. Salam and J. Strathdee , Nucl. Phys. B 87 (1975) 85 ; P. Fayet , Nucl. Phys. B 90 (1975) 104 .

53. CHARM Collab. F. Bergsma *et al.*, Phys. Lett. 121B (1983) 429.

54. P. R. Harrison and C. H. Llewellyn-Smith , Nucl. Phys. B 213 (1983) 223 ; B 223 (1983) 542(E) .

55. UA1 Collaboration , C. Albajar *et al.*, Phys. Lett. 198B (1987) 261 .

56. H. Baer and E. Berger , Phys. Rev. D 34 (1986) 1361 ; D 35 (1987) 406(E) ; E. Reya and D. P. Roy , Z. Phys. C 32 (1986) 615 .

57. R. M. Barnett , J. F. Gunion , H. E. Haber , Phys. Rev. D 37 (1988) 1892 .

58. J. Zuk , G. C. Joshi and J. W. G. Wignall , Phys. Rev. D 28 (1983) 1706 ; G. Eilam and A. Khare , Phys. Lett. 134B (1984) 269 ; W. Y. Keung and A. Khare, Phys. Rev. D 29 (1984) 2657 ; J. H. Kühn , Phys. Lett. 141B (1984) 433 ; J. H. Kühn and S.

Ono , Phys. Lett. **142B** (1984) 436 .

59. D. V. Nanopoulos , S. Ono and T. Yanagida , Phys. Lett. **137B** (1984) 363 .

60. A. N. Mitra and S. Ono , TH. 3707-CERN (1983) .

61. J. L. Richardson, Phys. Lett. 82B (1979) 272 ; E. Eichten, K. Gottfried, T. Kinoshita, J. Kogut , K. D. Lane and T.-M. Yan, Phys. Rev. Lett 34 (1975) 369 ; T. Applequist , A. De Rújula, H. D. Politzer and S. L. Glashow ; Phys. Rev. Lett. 34 (1975) 365 ; R. Levine and Y. Tomozawa ; Phys. Rev. D 21 (1979) 840; W. Buchmüller , G. Grunberg and S.-H.H. Tye, Phys. Rev. Lett. 45 (1980) 103 .

62. A. J. Buras , E. G. Floratos, D. A. Ross and C. T. Sachrajda, Nucl. Phys. B 131 (1977) 308 ; A. Billoire , Phys. Lett. 92B (1980) 343 ; W. Fischler, Nucl. Phys. B 129 (1977) 157 .

63. K. Igi and K. Hikasa , Phys. Rev. D 28 (1983) 565.

64. G. Bhanot and S. Rudaz , Phys. Lett. 78B (1978) 119 .

65. B. B. Deo and B. K. Barik , Phys. Rev. D 27 (1983) 249 .

66. A. K. Roy and S. Mukherjee , Pramana- J. Phys. 27 (1986) 761.

67. W. Kwong and J. L. Rosner , Phys. Rev. D 38 (1988) 279 .

68. L. P. Fulcher , Phys. Rev. D 39 (1989) 295 .

69. D. P. Roy , TIFR/TH/89-10 .

70. VENUS Collaboration : H. Yoshida *et al.*, Phys. Lett. **198B** (1987) 570 ; AMY Collaboration : H. Sagawa *et al.*, Phys. Rev. Lett. 60 (1988) 93 ; TOPAZ Collaboration : J. Adachi *et al.*, Phys. Rev. Lett. 60 (1988) 97 .

71. R. M. Godbole, S. Pakvasa and D. P. Roy , Phys. Rev. Lett. 50

(1983) 1539 ; V. Barger , A. D. Martin and R. J. N. Phillips, Phys. Rev. D 28 (1983) 145 .

72. UA1 Collaboration : C. Albajar *et al.*, Z. Phys. C 37 (1988) 505 .

73. D. P. Roy , Phys. Lett. 196B (1987) 395 ; H. Baer *et al.*, Phys. Rev. D 37 (1988) 3152 ; D. Atwood *et al.*, Phys. Rev. D 36 (1987) 1547 .

74. CDF , UA1 and UA2 Collaborations , Seminars given at CERN , April 18, 1989 .

75. S. Ghosh and S. Mukherjee , Mod. Phys. Lett. 4A (1989) 1277 .

76. W. Buchmüller and S.-H.H. Tye , Phys. Rev. D 24 (1981) 132 .

77. V. Kriss and B. Ram , Mod. Phys. Lett. 3A (1988) 33 .

78. V. Gupta and R. Kögerler , Phys. Rev. D 37 (1988) 740 .

79. K. Igi and S. Ono , Phys. Rev. D 36 (1987) 1550 ; D 37 (1988) 1338(E) .

80. J. Pantaleone, S.-H.H. Tye and Y. J. Ng , Phys. Rev. Lett. 55 (1985) 916 ; J. Pantaleone and S.-H.H. Tye , Phys. Rev. D 37 (1988) 3337 .

81. S. N. Gupta , S. F. Radford and W. W. Repko , Phys. Rev. D 34 (1986) 201 .

82. M. G. Olsson and C. J. Suchyta III , Phys. Rev. D 36 (1987) 1459 .

83. M. G. Olsson and C. J. Suchyta III , Phys. Rev. Lett. 57 (1986) 37 .

84. S. W. Otto and J. D. Stack , Phys. Rev. Lett. 52 (1984) 2328.

85. M. Lüscher , Nucl. Phys. B 180 (1981) 317 .

86. A. Martin , CERN-TH. 4161/85 .

87. S. Jacobs , M. G. Olsson and C. Suchyta III , Phys. Rev. D 33 (1986) 3338 .

88. S. N. Gupta, W. W. Repko and C. J. Suchyta III , Phys. Rev. D 39 (1989) 974 .

89. S. Schmitz , D. Beavis and P. Kaus , Phys. Rev. D 36 (1987) 184 .

90. K. J. Sebastian , H. Grotch and X. Zhang , Phys. Rev. D 37 (1988) 2549 .

91. S. Ghosh and S. Mukherjee , Mod. Phys. Lett. 4A (1989) 2667 .

92. S. Ghosh and S. Mukherjee , paper contributed to Europhysics HEP Conference (Madrid) 1989 .

93. R. K. Bhaduri , L. E. Cohler and Y. Nogami , Phys. Rev. Lett. 44 (1980) 1369 .

94. D. P. Stanley and D. Robson, Phys. Rev. D 21 (1980) 3180 ; S. Godfrey and N. Isgur , Phys. Rev. D 32 (1985) 189 .

95. S. Ono and F. Schöberl , Phys. Lett. 118B (1982) 419 .

96. S. N. Gupta , Phys. Rev. D 35 (1987) 1736 .

97. S. Ghosh , A. K. Roy and S. Mukherjee , Mod. Phys. Lett. 2A (1987) 183 .

98. H. Grosse and A. Martin , Phys. Rep. C 60 (1980) 341 and references therein .

99. R. D. Schamberger *et al.*, Phys. Lett. 138B (1984) 225 ; S. E. Csorna *et al.*, Phys. Rev. Lett. 56 (1986) 1222 ; H. Albrecht *et al.*, DESY 87-087 .

100. J. L. Rosner , C. Quigg and H. B. Thacker , Phys. Lett. 74B

(1978) 350 ; C. N. Leung and J. L. Rosner , J. Math. Phys. 20 (1979) 1435 .

101. J. Ellis and H. Kowalski , Phys. Lett. 142B (1984) 441 ; 157B (1985) 437 ; G. Altarelli , B. Mele and S. Petrarca , Phys. Lett. 160B (1985) 317 ; H. Albrecht *et al.*, (The ARGUS Collaboration) Phys. Lett. 167B (1986) 360 .

102. T. Goldman and H. E. Haber , Physica D 15 (1985) 181 .

103. A. Martin , Phys. Lett. 70B (1977) 192 .

104. L. Brink and J. H. Schwarz , Nucl. Phys. B 121 (1977) 285 .

105. G. L. Kane and J. P. Leveille , Phys. Lett. 112B (1982) 227 .